國立臺灣大學工學院化學工程學系

碩士論文

Graduate Institute of Chemical Engineering

College of Engineering

National Taiwan University

Master Thesis

單寧酸/多面體矽氧烷寡聚物改質疏水化棉布進行油水分離

Hydrophobicity modification for cotton fabrics by tannic acid/POSS for oil/water separation

林子傑

Tzu-Chieh Lin

指導教授：李篤中 博士

Advisor: Duu-Jong Lee, Ph.D.

中華民國 110 年 7 月

July, 2021

doi:10.6342/NTU202101615

ACKNOWLEDGEMENTS

First and foremost, I sincerely thank to my advisor, Dr Duu-Jong Lee for guiding and supporting me. In these two year, I learned how to do the research and present the data logically from Dr Lee. Furthermore, my English skill was improved because of numerous English presentations. All the experience I have learned from graduate school are beneficial.

Secondary, I am grateful to my lab members. For lab mate: Lai Yan-Ru and Huang Wei-Hao, thanks for your assistance and company. For lab juniors: Liao-Jun Bo and Huang-Wei Hao, Thanks for your assistance in the experiment. For lab assistance: Ho Mi-Ni and Chang Ying-Ju, thanks for your help in administrative affairs.

Finally, I want to express my sincerest gratitude to my family and friend. for supporting me to finish my master degree. I will keep hard working to accomplish my goal in the future.

doi:10.6342/NTU202101615

ABSTRACT

This article provides a perspective review on the use of modified cotton fabrics for oil-water separation. The principles of surface hydrophobicity of cotton fabrics are first described, from which the basis for producing superhydrophobic surfaces is presented. Then the preparation methods to convert hydrophilic cotton fabrics to hydrophobic fabrics are reviewed and discussed. Based on literature results the way to design novel preparation methods, the need to summarize testing protocols, and the comprehensive technoeconomic and sustainability analyses, are proposed. A demonstrative cotton fabrics test is used to reveal the significant role of conjugated fluid flows and surface interactions under different application scenarios for determining the separation efficiency of the oil-water mix.

POSS-modified cotton fabric named as POSS-CT is synthesized through thiol-ene click reaction showing rough and hydrophobic surface with 142.82±1.17° of water contact angle. POSS-CT possesses 0.96 g/g of oil absorption capacity for floating oil cleanup which is almost 3 times higher the pristine cotton fabric.

TA-ODA, TA-HDA and TA-TDA are fabricated by crosslinking tannic acid (TA) with octadecylamine (ODA), hexadecylamine (HDA) and tetradecylamine (TDA) through Michael addition/Schiff base reaction in one step, respectively. Moreover, 60 min of the modification with 5mM $CuSO_4$ and 19.6mM H_2O_2 represent 142.87±0.53°, 135.99±1.15° and 133.27±1.15° of water contact angle which are decreased as the dreceasing length of alkylamine. TA-ODA, TA-HDA and TA-TDA possess 1.01 g/g, 1.00 g/g and 0.96 g/g of oil absorption capacity representing outstanding floating oil cleanup capability as well as POSS-modified cotton fabric.

doi:10.6342/NTU202101615

Compared to POSS-modified cotton fabric, tannic acid-modified cotton fabrics are more suitable for practical application because of their low costs, simple fabrication process and sustainable solvent medium.

Keywords: Cotton fabrics; hydrophobicity; tannic acid; alkylamine; POSS; oil/water separation; testing

doi:10.6342/NTU202101615

摘要

本文對改質棉布應用在油水分離提供了觀點回顧。 首先描述了棉布表面疏水性的原理並介紹了產生超疏水表面的基礎理論。 然後對親水性棉布改質為疏水性棉布的製備方法進行了回顧和討論。本文提出了根據文獻結論設計出的新製備方法、總結測試方法、全面技術經濟以及永續性分析的必要性。棉布測試展示了流體和表面相互作用在不同應用場景下對確定油水混合物分離效率的重要關鍵。

POSS 改質棉布又稱為 POSS-CT 是通過硫醇-烯加成反應合成，表現出粗糙與水接觸角為 142.82±1.17°的疏水表面。POSS-CT 用於清除浮油具有 0.96 g/g 的吸油能力幾乎是純棉布的 3 倍。

單步驟製備的 TA-ODA、TA-HDA 和 TA-TDA 是用單寧酸 (TA) 與十八烷基胺 (ODA)、十六烷基胺 (HDA) 和十四烷基胺 (TDA)透過麥可加成/希夫鹼反應分別鍵結。 此外，用 5mM $CuSO_4$ 和 19.6mM H_2O_2 改質 60 分鐘表現出 142.87±0.53°、135.99±1.15°和 133.27±1.15°的水接觸角，水接觸角隨著烷基胺長度的減少而降低。 TA-ODA、TA-HDA 和 TA-TDA 擁有 1.01 g/g、1.00 g/g 和 0.96 g/g 吸油量表現出和 POSS 改質棉布一樣出色的浮油清除能力。

與 POSS-CT 相比，單寧酸改質棉布成本低、製造流程簡單、合成溶劑具永續性，更適合於實際應用。

關鍵字: 棉布; 疏水性; 單寧酸; 烷基胺; POSS; 油水分離; 測試

doi:10.6342/NTU202101615

Contents

doi:10.6342/NTU202101615

doi:10.6342/NTU202101615

doi:10.6342/NTU202101615

doi:10.6342/NTU202101615

List of Figures

doi:10.6342/NTU202101615

doi:10.6342/NTU202101615

doi:10.6342/NTU202101615

List of Tables

doi:10.6342/NTU202101615

Chapter 1
Introduction

Recently, oil spilling from livelihood, industry and accident cause damage to the environment and ecosystem, which has great influence on wildlife and human health [1]. The oil skimmer, centrifugation and air flotation have been developed to solve the oil spilling problem [2-5]. However, these traditional methods have drawback including low separation efficiency, high energy requirement and time-consuming procedures [6,7]. Cotton, a promising porous sorbents, is beneficial to deal with oil pollution because of its absorption capacity, sustainability, and low cost [8]. In this case, the hydrophobicity modification of cotton fabrics has been adopted to remove the oil pollution due to its ease operation and low processing cost [9, 10].

Hydrophobic material exhibits excellent water repellent property and consequently has been used to separate oil from water [11]. Grafting long chain alkyl compound [12], immobilizing polymer [13] and depositing nanoparticles [14] are performed to construct hieriarchical structure and reinforce the surface roughness to fabricate hydrophobic surface with low surface energy [15]. Moreover, the hydrophobicity can be enhanced by grafting the increased length of hydrocarbon [16].

Numerous modification protocols were proposed for surface modification. The in situ crosslinking reactions are adopted for surface hydrophobization [17, 18]. The cotton surface hydrophobized by grating with polyhedral oligomeric silsesquioxane (POSS) via thiol-ene reactions under UV irradiation has received research attention

doi:10.6342/NTU202101615

[19]. The chemistry involves conversion of the hydroxyl groups on cotton surface to thiol groups by thiol-containing silane, then adding POSS to react with the so-yielded thiol groups to form single bond by thiol-ene click reactions [19]. POSS are hybrid clusters with chemical formula $(RSiO_{1.5})_n$ [20], which is highly hydrophobic with poor affinity to water.

Natural inspired method has extensively been introduced to diverse applications owing to its post-funtionalization, mild reaction environment and adhesive ability [21, 22]. Hydrophobicity modification of natural inspired protocol is adopted to deal with oil spilling problem through oil/water separation. For instance, Li et al. [23] constructed dopamine-based hydrophobic coating on cotton fabric demonstrating good oil/water separation capability. Yan et al. [24] grafted dopamine hybrid coating with long chain alkyl amine to fabricate superhydrophobic cotton fabric representing great absorption capacity for organic solvent. Compared to dopamine (DA), tannic acid (TA) is a relatively inexpensive natural polyphenols (Table1) that can also serve as a satisfactory linker between surface and the grafted molecules [25], with the latter being achieved by reacting the excess catechol groups with amino-containing silane through Michael addition/Schiff base reactions [26]. However, the reaction time for grafting reactions with TA is generally long, 25 h for TA/Fe/ODA composite [27], and 36 hr for the TA/APTES/ODA composite [28], which should be significantly reduced for economy production (Table 2).

This study proposed a novel scheme for cotton surface modification with TA dip coating followed by long-chain alkylamine grafting via Michael addition/Schiff base reaction. The modification with TA can have a reduced cost compared with that with expensive DA. To accelerate the reaction for second reaction with alkylamine, the catalysts ($CuSO_4/H_2O_2$) proposed by Sun [30], which used the yielded film as

doi:10.6342/NTU202101615

slow-release carrier for fertilizer, were adopted. The cotton fabrics modified by the revised, one-pot modification scheme were demonstrated to exhibit superhydrophobic surfaces with satisfactory oil adsorption capability. To demonstrate the impact of chain length of alkylamine, tetradecylamine (TDA), hexadecylamine (HDA), and octadecylamine (ODA) were applied in this study for cotton fabrics modification. Furthermore, the hydrophobic cotton fabric coated with high cost of POSS is introduced to make a comparison with tannic acid-modified fabrics to realize the performance for oil/water separation which is fabricated through thiol-ene click reaction (Table 3).

Table 1. The comparison of price for dopamine hydrochloride and tannic acid

Substance	Brand	Pack size	Price (NTD/g)
Dopamine hydrochloride (98%)	Sigma-Aldrich	100g	198
Tannic acid (ACS reagent grade)	Sigma-Aldrich	100g	18
Tannic acid (Industrial grade, 67.5%)	Emperor Chemical	500g	0.34

Data from Sigma-Aldrich and Emperor Chemical

doi:10.6342/NTU202101615

Table 2. The comparison of reaction conditions for TA grafting modification tests

Substrate	Material*	Reaction	Procedure	Reaction time	Method	Contact angle (°)	Reaction condition	Ref.
PVDF membrane/ PES membrane	CA- $PEtO_x$ ($CuSO_4/H_2O_2$)	pH-induced reaction/oxidant-triggered rxn	One step	0.5 hr	Dip coating	54.5±0.3/73.5±1.9	Room temp.; pH 8.5	[29]
PTFE membrane/	TA-ODA ($CuSO_4/H_2O_2$)	Michael add rxn/Schiff base rxn/oxidant-triggered rxn	One step	10 min	Spray coating	124.5±4	55 ◦C	[30]
Cotton fabric	TA-Fe-ODA	Michael add rxn/Schiff base rxn	Two step	1st step: 1 hr 2nd step: 24 hr	Dip coating	145.35 ± 0.4	1st step: pH 8.0, room temp; 2nd step: pH 8.5, room temp	[27]
Cotton fabric	TA-APTES-ODA	Michael add rxn/Schiff base rxn	Two step	1st step: 24 hr; 2nd step: 12 hr	Dip coating	152	1st step: pH 8.5, room temp; 2nd step: pH 8.5, room temp	[28]
Cotton fabric	TA-ODA; TA-HDA; TA-TDA ($CuSO_4/H_2O_2$)	Michael add rxn/Schiff base rxn/oxidant-triggered rxn	One step	10 min	Dip coating	139.67±1.07° 133.05±1.54° 130.77±1.65°	Room temp., pH 8.5	This work

*CA: caffeic acid; $PEtO_x$: poly(2-ethyl-2-oxazoline); PTFE: polytetrafluoroethylene; TA: tannic acid; ODA: octadecylamine; APTES: (3-aminopropyl)triethoxysilane; GA: gallic acid

Table 3. The comparison of price for long chain alkyl compound, POSS, and MPTES

Substance	Brand	Price
Octadecylamine (90%)	ACROS Organics	0.093 ($/g)
Hexadecylamine (90%)	ACROS Organics	0.100 ($/g)
Tetradecylamine (98%)	ACROS Organics	3.622 ($/g)
Octavinyloctasilasesquioxane (POSS)	TCI	51 ($/g)
(3-Mercaptopropyl)triethoxysilane (MPTES)	Sigma-Aldrich	4.86 ($/ml)

Data from ACROS Organics, Tokyo Chemical Industry (TCI) and Sigma-Aldrich

doi:10.6342/NTU202101615

Chapter 2
Literature review

2.1 Hydrophobicity

In nature, the phenomena of the lotus leaf effect [31], rose petal effect [32] and butterfly wing effect [33] (Figure 2-1) have inspired people due to the promising application involving self-cleaning property [34], anti-adhesion ability [35] and hydrophobicity [36]. The hydrophobicity of lotus leaf is attributed to the hierarchical structure [37] which the air will be trapped into the rough structure to minimize the contact area between air and water droplet [38]. Consequently, the re-entrant structures of modified surface are performed to repel water out of the surface owing to the enhancement of hydrophobization [39, 40]

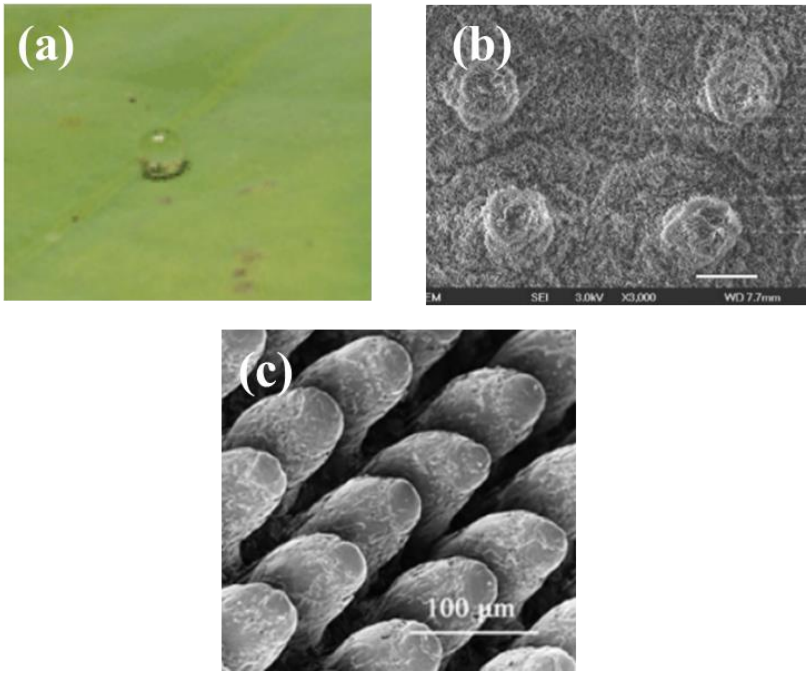

doi:10.6342/NTU202101615

Figure 2-1. The image (a) of the lotus leaf effect [31]. SEM image of lotus-leaf-like structures (b) from carbon nanotubes [31] and rose-petal-like structure (c) of modified surface [32].

2.2 The evaluation of surface energy of hydrophobicity

The hydrophobicity is contributed to the surface energy of the substrate and can be evaluated by measuring the contact angle [41]. When the droplet attaches on the solid material with a smooth surface, we can estimate the surface energy at three phase contact line through the Young equation (1) [42].

$$\gamma_L \cos\theta = \gamma_s - \gamma_{sL} \qquad (1)$$

where γ_L, γ_S, and γ_{SL} refers to the interfacial interaction between liquid and vapor (surface energy of liquid), the surface energy of solid material and the interfacial interaction between solid and liquid respectively. The contact angle (θ) is evaluated by the angle between solid and a liquid droplet on the surface (Figure 2-2)

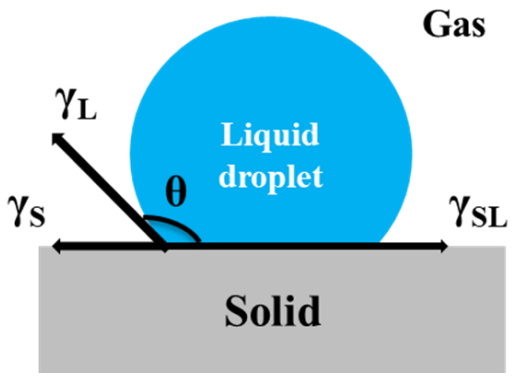

Figure 2-2. Schematic of three phase contact line

doi:10.6342/NTU202101615

When the static contact angle θ is higher than 90°, it can be normally called a hydrophobic surface by definition [43]. According to the equation, low γ_S can lead to high θ which indicates the low surface energy material is not readily to be attached by the high surface tension liquid [44]. Moreover, low γ_S represent the low polar and dispersive component of surface energy. The surface energy is ascribed to the sum of polar component and the dispersive component of surface energy (2) through Fowkes theory [45]

$$\gamma_s=\gamma_s^p+\gamma_s^d \qquad (2)$$

γ_s = the surface energy of solid

γ_s^p = the polar component surface energy of solid

γ_s^d = the dispersive component surface energy of solid

In Fowkes method, the interfacial interaction γ_{SL} is expressed as a geometric mean of polar (non-dispersive) and dispersive component [46]. The Fowkes method is shown in the following equation (3).

$$\gamma_{sL} = \gamma_S + \gamma_L - 2\left(\sqrt{\gamma_L^d.\gamma_s^d} + \sqrt{\gamma_L^p.\gamma_s^p}\right) \qquad (3)$$

γ_L^d = the dispersive component surface energy of liquid

γ_s^d = the dispersive component surface energy of solid

γ_L^p = the polar component surface energy of liquid

γ_s^p = the polar component surface energy of solid

doi:10.6342/NTU202101615

Combining the Young equation with the Fowkes method [47], we can get the equation (4).

$$\frac{\gamma_L(1+\cos\theta)}{2\sqrt{\gamma_L^d}} = \sqrt{\gamma_s^p}\left(\frac{\gamma_L^p}{\gamma_L^d}\right) + \sqrt{\gamma_s^d} \qquad (4)$$

Based on the above equation, the estimation of γ_s^d and γ_s^p can be determined by measuring the contact angle with two different liquids [48]. After that, the surface energy is subsequently obtained from the sum of the dispersion component and the polar component of surface energy.

2.3 The characteristic of cotton

Cotton is composed of cellulose (Figure 2-3) [49] which is cost-effective to be used as an oil adsorbent and biodegradable to the environment [50]. Moreover, it is beneficial to be modified by the functional group because of numerous hydroxyl groups on the pristine cellulose [51]. Overall, cotton has been considered as a promising substrate to solve oil spilling due to its absorption capacity, sustainability, and low cost [52].

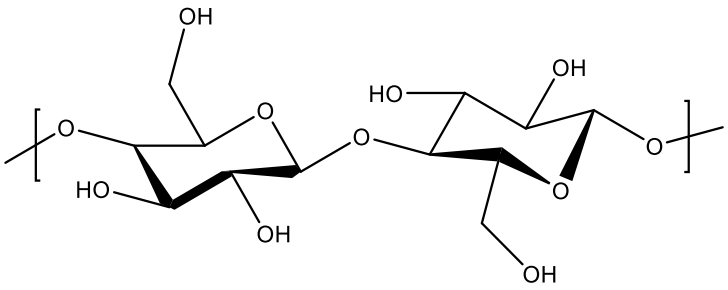

Figure 2-3. The chemical structure of cotton

doi:10.6342/NTU202101615

2.4 Hydrophobicity modification of cotton fabric for oil/water separation

Hydrophobicity modifications are introduced to impact the wettability of cotton fabric to deal with the oil spilling problem [53, 54]. The hydrophobization of the surface can be modified by various protocols including dip coating [55], in situ crosslinking reaction [56], UV-triggered reaction [57] and natural inspired method [58]. For instance, Liu et al. [59] deposited SiO_2 nanoparticles via dip coating to fabricate superhydrophobic cotton which could easily collect the floating oil. Zhang et al. [60] immobilized modified-ZnO/polystyrene on cotton fabric through dip coating to synthesize superhydrophobic cotton fabric possessing high oil/water separation efficiency (Figure 2-4). Deposition of nanoparticles, such as SiO_2 [61], ZnO [62] and TiO_2 [63], are introduced to hydrophobization owing to the reinforcement of surface roughness [64]. In addition, the doping of polymers is also utilized to the formation of hydrophobization [65]. Cao et al. [66] synthesized PDMS-ormosil-based superhydrophobic fabric for oil removal from the emulsion solution. Guo et al. [67] modified cotton fabric with the polymerization of PDMS, FAS15 and PVP to separate water-in-oil emulsion driven by gravity. The key of hydrophobicity is ascribed to the low surface energy of polymer compounds [68]. Furthermore, grafting long chain alkyl substances, such as alkylamine [69], alkylsilane [70] and fluoroalkylsilanes [71], has been extensively adopted to develope the hierarchical structure [72] (Figure2-5). A superhydrophobic cotton fabric coated with trimethoxy(octadecyl)silane exhibited high oil absorption performance under the water [73]. The decreasing surface energy can be synergistically modified with the increased alkyl chain length to construct a re-entrant structure [74].

doi:10.6342/NTU202101615

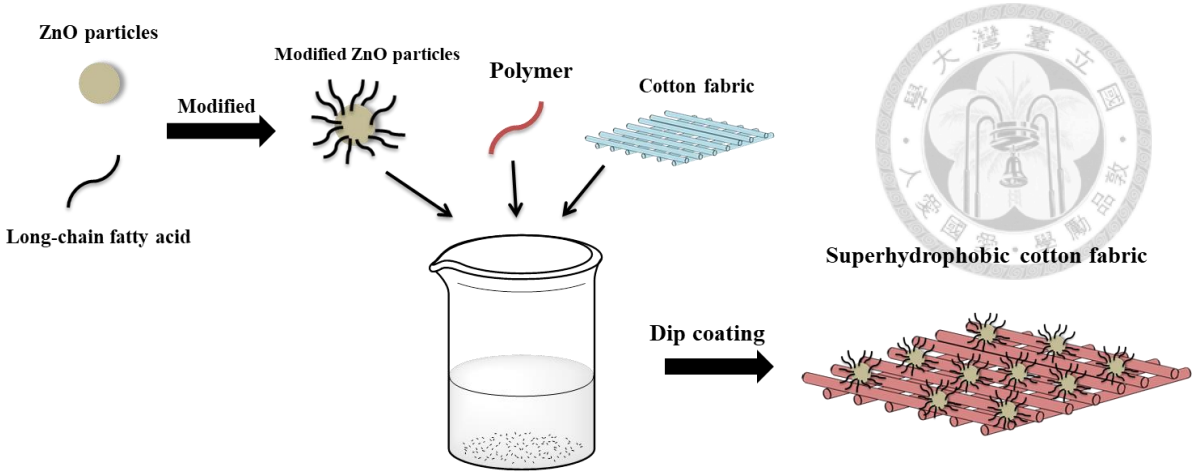

Figure 2-4. Schematic of fabrication of superhydrophobic cotton fabric via dip coating [60]

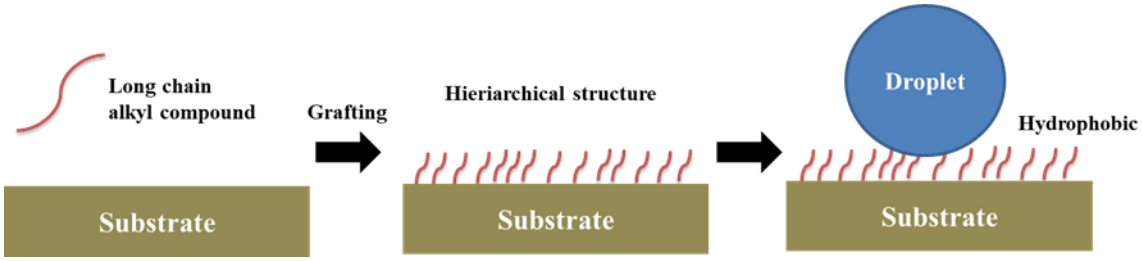

Figure 2-5. Schematic of formation of hierarchical structure by grafting long chain alkyl compound

2.5 Natural inspired method

Nature-inspired method has received great attention due to its sustainability, flexibility, and versatile application[58]. Scientists found dopamine from mussel possessing adhesive ability [75] and can polymerize spontaneously into polydopamine (pDA) in the mild environment [76] without using UV-induced reaction [77] and plasma-induced reaction [78] required expensive equipment. Dopamine (DA) is promising for surface modification due to multifunctional group (catechol and amino

doi:10.6342/NTU202101615

groups) [79] and also act as a binder for further modification [80]. Zhao et al. [81] constructed dopamine-modified antifouling membrane for water purification. Zeng et al. [82] utilized dopamine to fabricate hydrophilic surface to prevent membrane blocking. Since the modification of membrane by dopamine perform hydrophilicity [83], these approaches are applied to prevent the membrane fouling attributed to the interaction between membrane and foulant [84]. In contrast with the hydrophilicity modification, hydrophobization of surface is also developed by the application of dopamine. For instance, dopamine-based hydrophobic film was built on the copper surfaces to enhance the corrosion resistance [85]. Yan et al. [24] adopted Fe/pDA/ODA-modified cotton fabric for oil/water separation. Dan et al. [86] fabricated dopamine-assisted superhydrophobic cotton through Schiff base reaction. The secondary reaction of polydopamine (pDA) coating can be modified via grafting of macromolecules [87], deposition of long-chain molecules [85, 86], and reduction of metal ions [76]. However, the high cost of dopamine is hard to find practical applications [88,89]. (Table 1) Compared to dopamine, tannic acid also shows excellent adhesion on various substrates [90] and is a cost-effective compound [91].

Tannic acid (TA) is a kind of natural polyphenols which possess abundant catechol functional groups [92] (Figure 2-6). Since tannic acid exhibit outstanding antibacterial [93] antioxidant performance [94], versatile applications such as food packaging [95], biomedical material [96] and antibacterial membrane [97] have been widely used. Furthermore, tannic acid is acted as a crosslinker [98, 99]. Xu et al. [100] utilized tannic acid to react with polyamine via co-deposition on nanofiltration membrane. Li et al. [101] constructed antifouling layer on membranes attributed to the co-deposition of tannic acid and polyethyleneime. Lin et al. [102] crosslinked tannic acid with piperazine via interfacial polymerization for dye/salt separation application. Tannic

doi:10.6342/NTU202101615

acid is enable to co-deposit with amine [103, 104] via Michael addition/Schiff base reaction and coordinate with metal ions (Figure 2-7) [105]. For instance, Xu et al. [106] developed tannic acid-modified coating via Michael addition/Schiff base reaction to prevent biofouling. The catechol groups of tannic acid will oxidize into reactive quinone structures and further react with amine through Michael addition/Schiff base reaction [30] (Figure 2-8). Tannic acid is also introduced to construct hydrophobic surface because of the hierarchical structure which is essential to the hydrophobization [107] (Figure 2-9). Sun et al. [30] adopted tannic acid-based hydrophobic film reacting with octadecylamine via co-deposition. Bu et al. [108] grafting fluorinated thiol on tannic acid-modified textile to form the superhydrophobic surface. Shang et al. [109] introduced polyhedral oligomeric silsesquioxane to crosslink with tannic acid to fabricate superhydrophobic cotton fabric for oil/water separation. Secondary modification of grafting of long chain alkyl compound [28], fluorine-containing substance [108] and polyhedral oligomeric silsesquioxane [109] are used for hydrophobization of tannic acid-derived substrate (Figure 2-10).

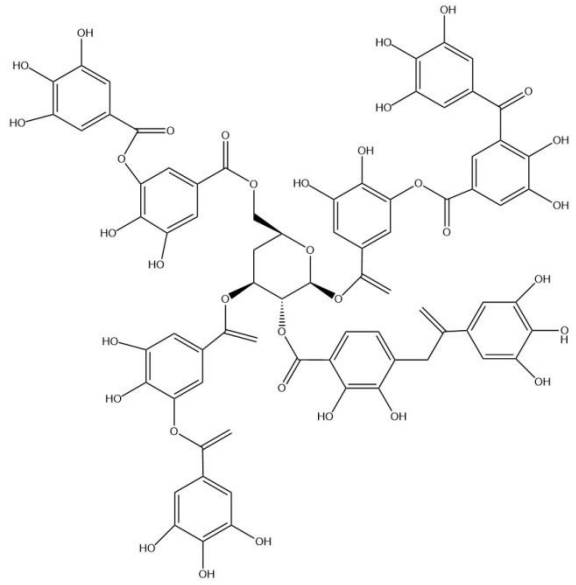

Figure 2-6. The structure of tannic acid

doi:10.6342/NTU202101615

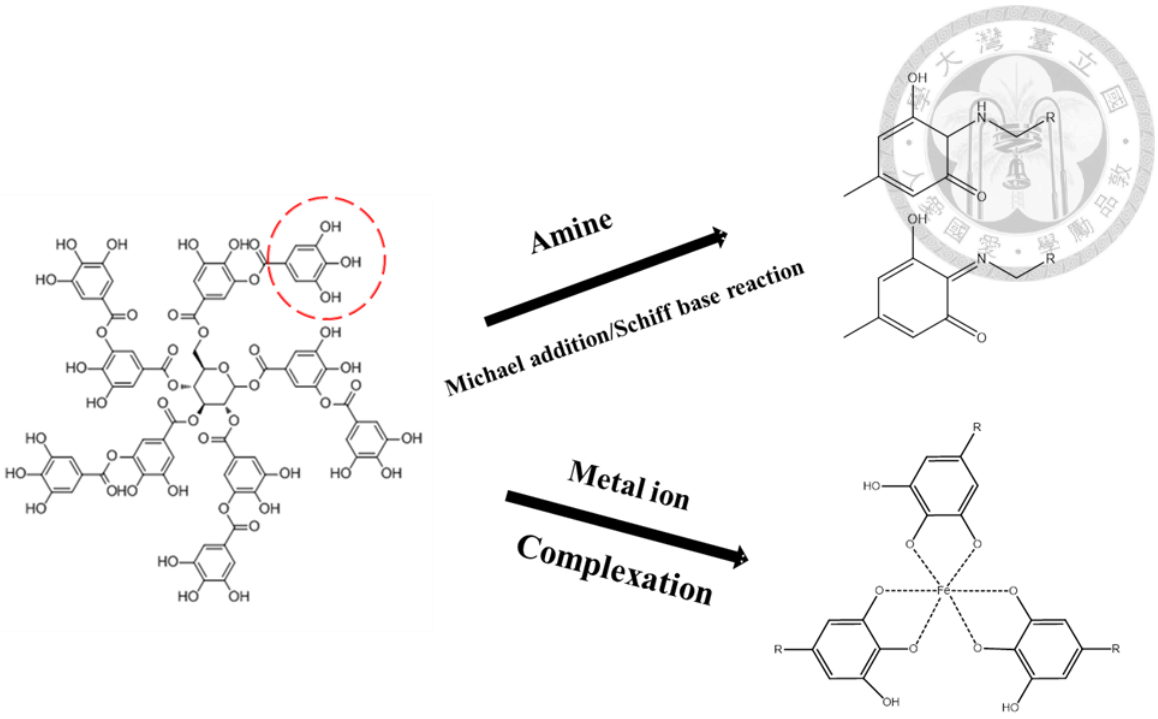

Figure 2-7. Schematic of complexation and Michael addition/Schiff base reaction for tannic acid

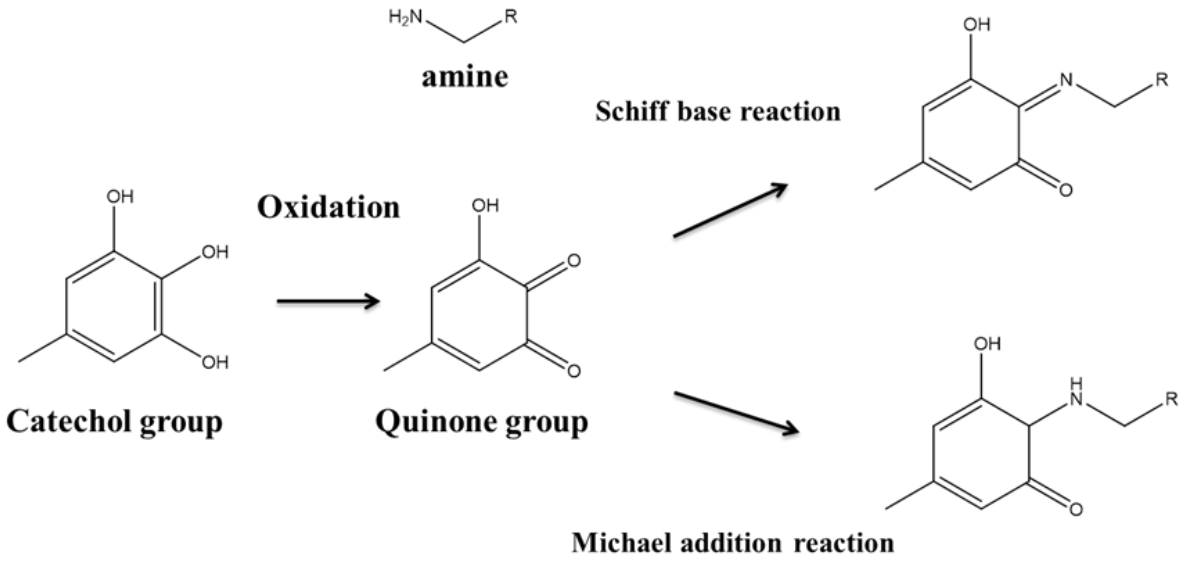

Figure 2-8. Mechanism of Michael addition/Schiff base reaction between tannic acid and amine

doi:10.6342/NTU202101615

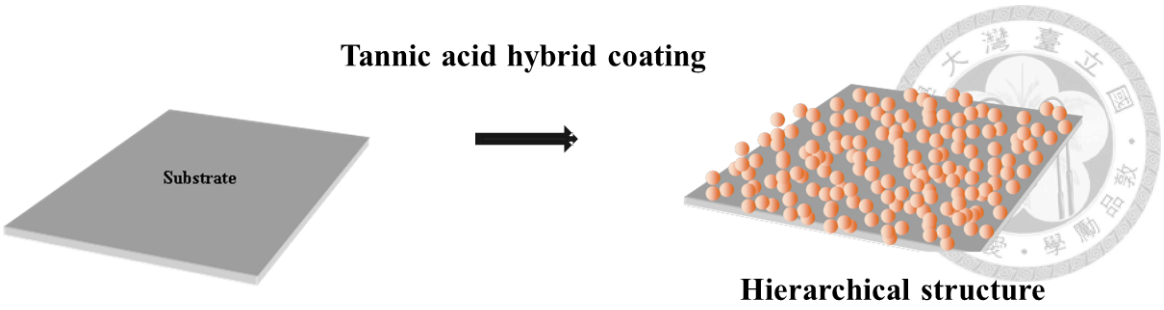

Figure 2-9. Schematic of hierarchical structure for tannic acid hybrid coating

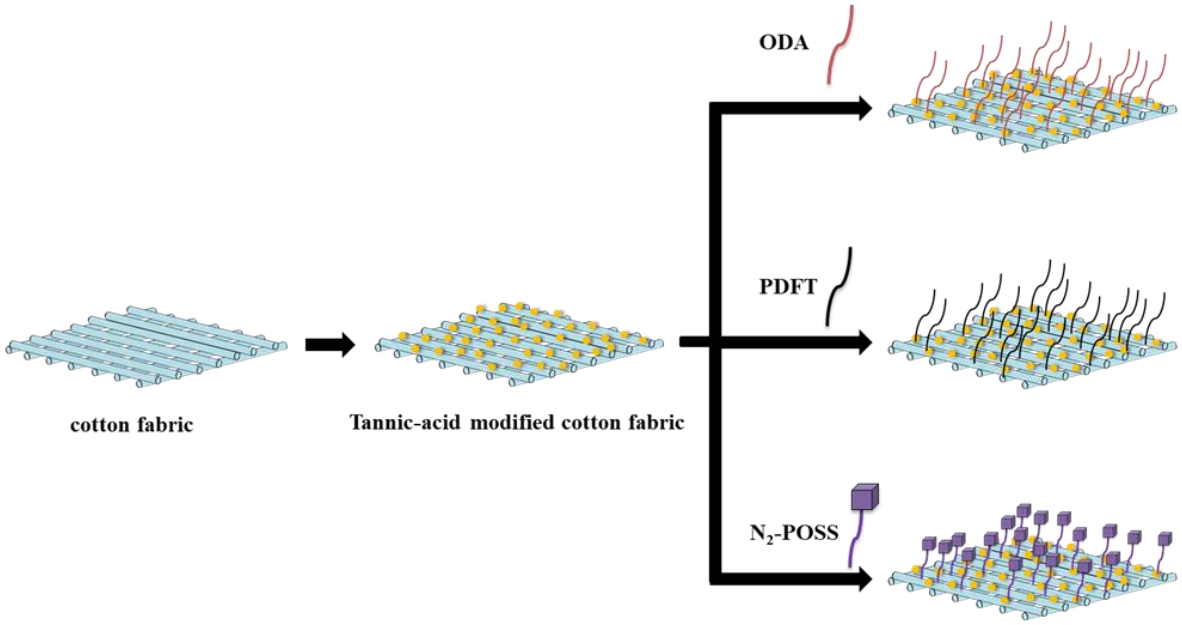

Figure 2-10. Schematic of secondary reaction for tannic acid-modified hydrophobic cotton fabrics [28, 108, 109]

doi:10.6342/NTU202101615

2.6. Michael addition reaction

Michael addition reaction, which is widely applied for click reaction, has attracted attention owing to the mild reaction condition [110], high yield production [111] and selectivity of reaction [112]. The Michael addition reaction is a reaction which the nucleophilic (Michael donor) will react with activated olefins and alkynes (Michael acceptor) [113], as shown in Figure 2-11. Numerous thiols [114], amines [115] and phosphine[116] can serve as Michael donor to react with Michael acceptor including ketones[117], α,β-unsaturated aldehydes[118] and azo compounds[119]. The application of Michael addition reaction is introduced to formation of polymer[120], immobilization of post-modification[121] and design for drug delivery system [122].

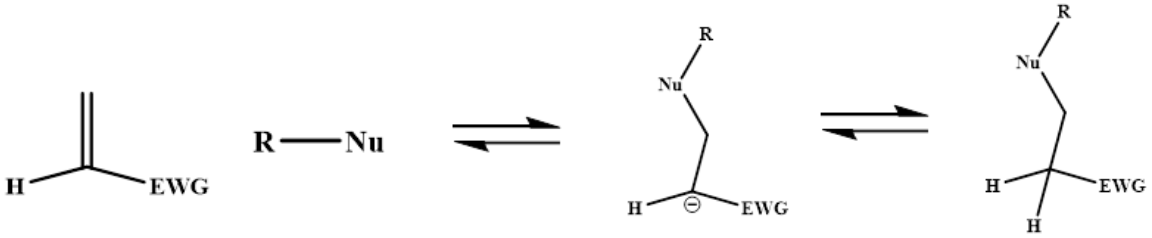

Figure 2-11. Schematic of Michael addition reaction [113]

2.7. Schiff base reaction

Schiff base reaction is adopted for biological application [123] as a result of the mild reaction condition [124], high reaction rate [125] and covalent bonding interaction [126]. Schiff base reaction refers to the reaction which the aldehydes (or ketones) will covalent with amino-containing compounds to form the imine groups [127] (Figure 2-12). Lui et al. [123] fabricated amino carboxymethyl chitosan-assisted hydrogel with biocompatibility property via Schiff base reaction. Xiang et al. [128] anchored tannic acid-based film on membrane via Schiff base reaction to prevent the

doi:10.6342/NTU202101615

fouling problem. Crosslinked biological materials based on Schiff base reaction has been widely adopted in the biomedical field [129].

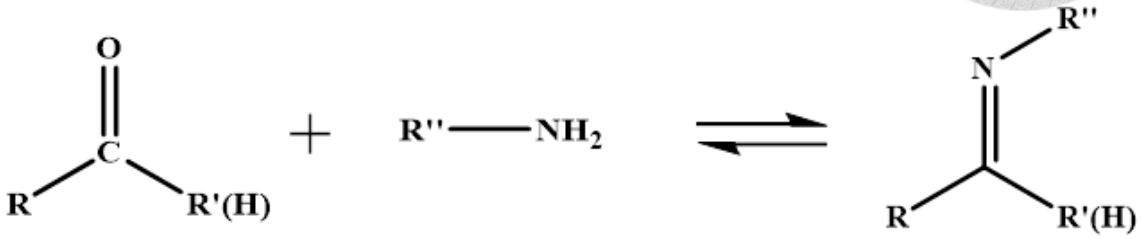

Figure 2-12. Schematic of Schiff base reaction [127]

2.8. $CuSO_4/H_2O_2$-triggered reaction

Nature inspired method is applied for surface modification owing to its post-functionalization [130], biocompatibility [131] and adhesion capacity[132]. Nevertheless, the reaction time of natural inspired method is time-consuming [133] compared to the UV- triggered protocol [134], in situ crosslinking method [135] and plasma-induced approach[136]. To overcome the drawback, numerous protocols have been developed. Xu et al. [137] utilized UV irradiation to produce the reactive oxygen species which promoted the polymerization of dopamine. Cai et al. [138] deposited the dopamine on TiO_2 nanotubes via electropolymerization to prevent the combination of electron-hole pairs. Lee et al. [139] introduced microwave irradiation to accelerate the rate of polymerization of dopamine. However, these instrument-required procedures are complicated and energy-consuming [140] which indicates the reaction consequently can not be utilized in large-scale production. In 2016, Zhang et al. [141] found that $CuSO_4/H_2O_2$ can act as a trigger to improve the deposition rate and homogeneity of polydopamine coating which required ten hours up to a few days to

doi:10.6342/NTU202101615

synthesize. Cu^{2+} and H_2O_2 are introduced to produce reactive oxygen species which act as the oxidant to accelerate the reaction rate of catechol groups of dopamine to reactive quinone structures [140] (Figure 2-13). Oxidant plays an important role to the oxidation reaction. Therefore, oxidant-assisted protocols are also introduced to enhance the copolymerization rate of polyphenol. For instance, tannic acid-assisted hydrophobization was induced by $CuSO_4/H_2O_2$ to enhance the polymerization rate [30]. He et al. [29] fabricated poly(caffeic acid)-derived hydrophilic coating with fast deposition rate through $CuSO_4/H_2O_2$-assisted reaction. Similar to the mechanism of oxidation of dopamine, the catechol structures of polyphenol are induced into quinone groups [29, 142] which applied $CuSO_4/H_2O_2$ to promote the rate of polymerization (Figure 2-14) [30]. The addition of $CuSO_4/H_2O_2$ reagent is adopted to optimize the deposition rate of polyphenol and reinforce the uniformity of coating [142, 29].

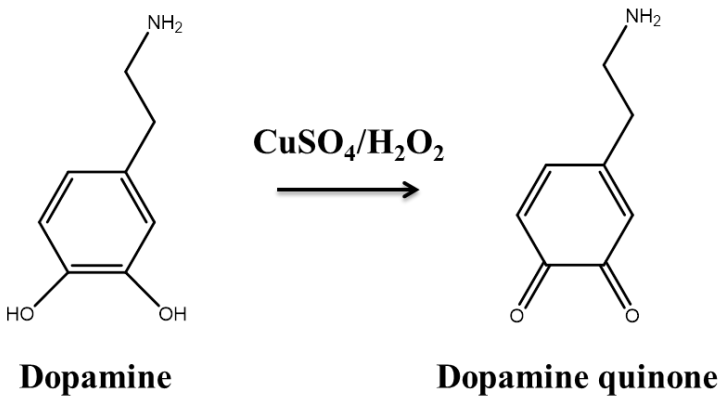

Figure 2-13. Schematic of $CuSO_4/H_2O_2$-triggered oxidation of dopamine

doi:10.6342/NTU202101615

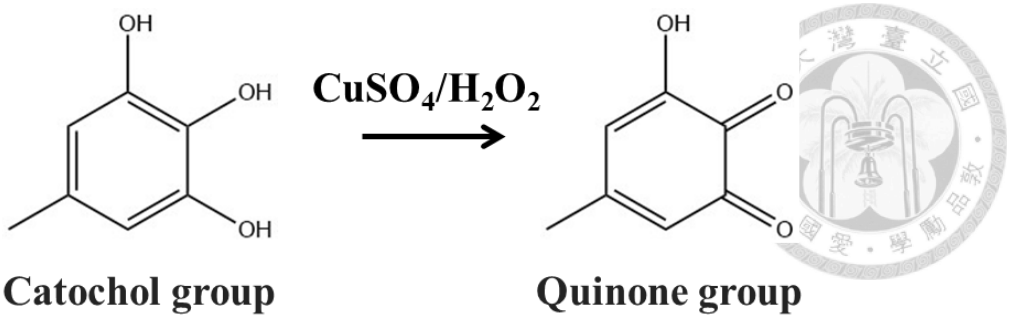

Figure 2-14. Schematic of $CuSO_4/H_2O_2$-triggered oxidation of tannic acid

2.9. Thiol-ene click reaction

Thiol-ene click reaction, a radical-mediated reaction, was capable of synthesizing functional materials rapidly with no by-products under mild reaction condition [143, 144]. Ke et al. [145] coordinated thiol-terminated polymer with $BaTiO_3$ nanoparticles through thiol-ene click reaction to prepare high energy storage material. Di et al. [146] adopted vinyl-POSS to react with thiol-modified cotton fabrics via thiol-ene click reaction to construct hydrophobic surface. Thiol groups are able to crosslink with ene induced by radical through thermo-initiated or photoinitiated thiol-ene click reaction (Figure 2-15) [147]. Photo-and thermal initiator, including 2,2-dimethoxy-2-phenylacetophenone (DMPA), 2-hydroxy-2-methylpropiophenone (HMPF) and 2,2'-azobis(isobutyronitrile) (AIBN), are frequently introduced to create the radical to induce the reaction [147, 148]. Lei et al. [149] applied DMPA as photoinitiator to trigger the polymerization between polymercaptopropylmethylsiloxane and vinyl-polydimethylsiloxane though thiol-ene click reaction. Amanda et al. [150] fabricated hexadecene-assisted superhydrophobic cotton fabric utilizing AIBA as initiator to derive the thermally initiated thiol-ene click reaction. Thiol-ene click reaction has been extensively conducted to surface

doi:10.6342/NTU202101615

modification [151], conjugation of polymer [152] and biofunctionalization of biomedical material [153].

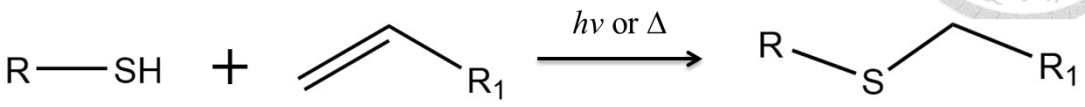

Figure 2-15. Schematic of thiol-ene click reaction

2.10. Polyhedral oligomeric silsesquioxane (POSS)

Polyhedral oligomeric silsesquioxane (POSS) possesses organic–inorganic hybrid cage-like nanostructure which are demonstrated the formula of $(RSiO_{1.5})_n$ (Figure 2-16) [154]. R can be composed of non-reactive groups such as methyl, isobutyl and phenyl [155]. On the contrary, R can be substituted by numerous reactive groups including vinyl, amine, styrene and thiol which are beneficial for further modification [155, 156]. Siyu et al. [157] fabricated POSS-assisted superhydrophobic cotton fabric which represented self-healing and outstanding anti-abrasion ability. Warintorn et al. [158] reinforced the strength and toughness of epoxy with rubber-derived POSS nanoparticles representing the impact resistance was enhanced 80%. POSS was conducted to improve the mechanism strength and chemical stability such as abrasion resistance, impact strength, corrosion resistance and UV resistance [159-161]. In addition, hydrophobicity modification is developed with application of POSS owing to the low surface energy [162, 57]. Choa et al. [163] developed superhydrophobic cotton fabric with POSS-constructed polymer exhibiting excellent durability and

doi:10.6342/NTU202101615

self-cleaning ability. POSS has functionalized the advanced material for widespread applications.

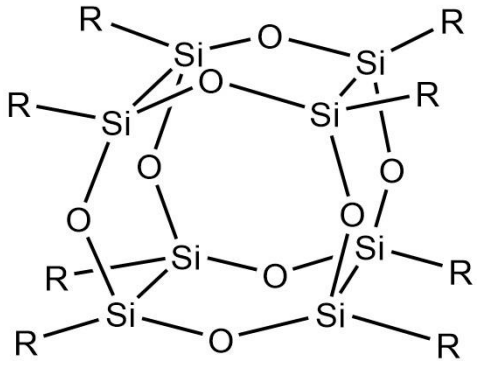

Figure 2-16. The chemical structure of POSS

doi:10.6342/NTU202101615

Chapter 3
Material and Experiment Methods

3.1. Materials

The cotton fabric was purchased from local cotton fabric store in Taipei, Taiwan. The long chain alkyl amine octadecylamine (ODA) (90%), hexadecylamine (HDA) (90%), tetradecylamine (TDA) (98%), copper sulfate (98+%), potassium bromide (KBr), n-hexane and diiodomethane were obtained from Fisher Scientific Int. Inc. (Pittsburg, PA, USA). Tannic acid, 2,2-Dimethoxy-2-phenylacetophenone (DMPA) and (3-Mercaptopropyl)triethoxysilane (MPTES), Dimethyl sulfoxide-d_6 (DMSO-d_6) and chloroform-d were purchased from MilliporeSigma (Burlington, MA, USA). Tris (Base) was obtained from J.T. Baker (Radnor, PA, USA). The hydrogen peroxide was purchased from Honeywell (Charlotte, NC, USA). Octavinyloctasilasesquioxane (POSS) was obtained from Tokyo Chemical Industry (TCI). Hydrochloric acid was obtained from Scharlau (Sentmenat, Spain). Ethanol (95%) was obtained from the Dinhaw Enterprise Co., Ltd. (Taipei, Taiwan). Dichloromethane was purchased from Shimakyu's Pure Chemicals Co., Ltd..

doi:10.6342/NTU202101615

3.2. Preparation of as-prepared cotton fabric

The as-prepared cotton fabrics were prepared by washing with deionized water and ethanol for three time, respectively. Then, immerse the cotton fabrics in the deionized water to do the ultrasonic treatment for about 30 minutes. After that, the cotton fabrics were dried in the oven at 60℃.

3.3. Fabrication of POSS-modified cotton fabric

The cotton fabrics were first immersed in the 0.15 mol/L MPTES of ethanolic solution for 2 hrs at ambient temperature. The modified fabrics were washed with ethanol and then dried at 60℃ to get the SH-CT. Afterward, SH-CT was immersed into the dichloromethane with 1.6 weighting percent of POSS and 0.16 weighting percent of DMPA under the 360 nm UV lamp reacting for 1 hour. Finally, wash the POSS-modified fabric with ethanol and dry the fabric at 60℃ to obtain the POSS-CT. (Figure 3-1)

3.4. Fabrication of tannic acid-modified cotton fabrics

Tannic acid (2 mg/ml) and $CuSO_4$ (5 mM)/H_2O_2 (19.6 mM) was added into the deionized water with strong stirring. At identical molar concentrations, ODA (3.33 mg/ml), HDA (2.97 mg/ml) or TDA (2.42 mg/ml) were individually dissolved in ethanol assisted with ultrasound. Then mix tannic acid/$CuSO_4$/ H_2O_2 solutions with the alkylamine/ethanol solution at room temperature, using $CuSO_4$/H_2O_2 to accelerate the oxidization of catechol groups. Subsequently, Tris and HCl were applied to adjust the solution pH to 8.5 to promote the Michael addition/Schiff base reactions. Finally, the cotton fabrics were dipped into the solution for 60 min at ambient temperature. After dipping the cotton fabrics were washed with water and ethanol and then dried at 60 ℃ to yield the products TA-ODA, TA-HDA or TA-TDA cotton fabrics. (Figure 3-2)

doi:10.6342/NTU202101615

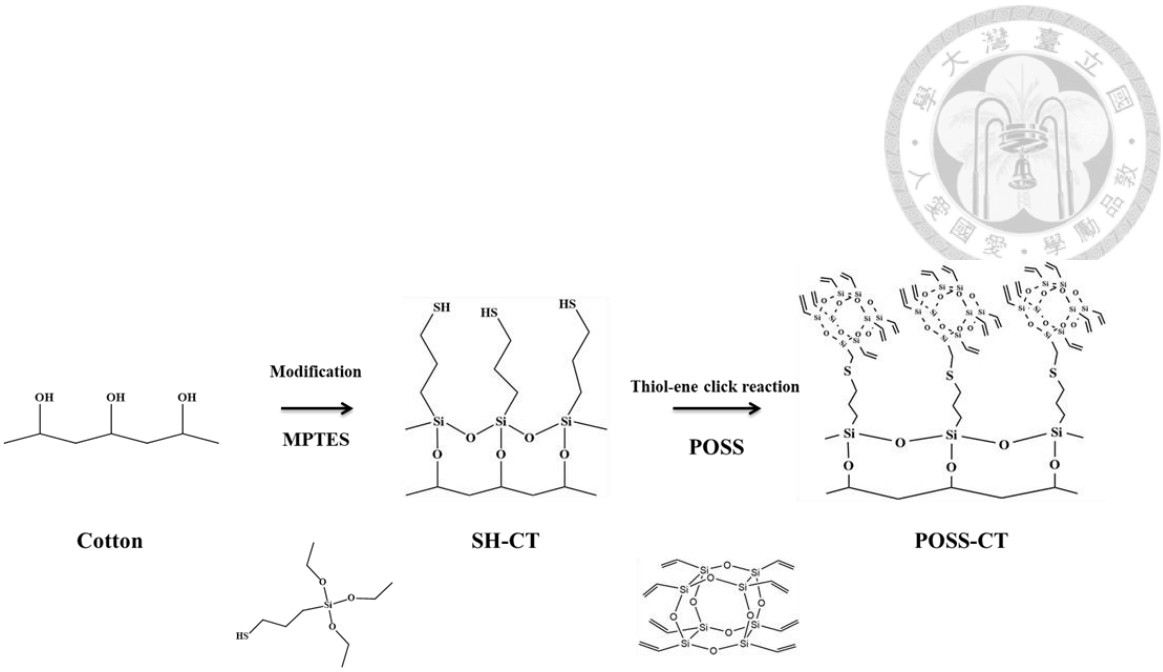

Figure 3-1. Schematic of two stage fabrication process of POSS-CT.

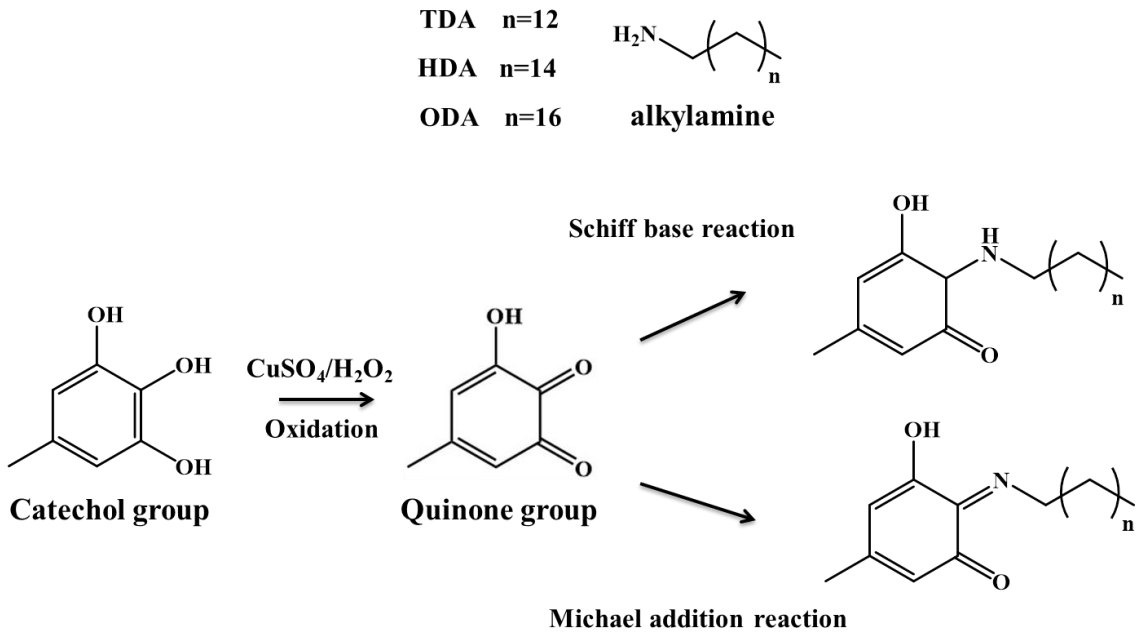

Figure 3-2. Schematic of the adopted reactions in this work. The two step reactions were performed in the same reactor to establish one-pot modification

doi:10.6342/NTU202101615

3.5. Characterization and instrumentation

3.5.1 Fourier Transform Infrared Spectroscopy (FTIR)

The functional groups of cotton fabric, tannic acid-modifed cotton fabric and POSS-modified cotton fabric were measured for 4 times by (Perkin Elmer, Waltham, MA, USA) from wavenumber 4000 to 450 cm^{-1}. Before measurement, the samples were dried in 40℃ vacuum oven overnight.Then the samples were mixed with potassium bromide (KBr) for measurement.

3.5.2 Nuclear Magnetic Resonance (NMR)

The ^{1}H NMR spectra was tested by AVIII-500 (Bruker, Billerica, MA, USA). Tannic acid was dissolved in DMSO-d_6 and ODA, HDA, TDA, POSS, MPTES were dissolved in $CDCl_3$. The sample preparation of TA-ODA, TA-HDA and TA-TDA were prepared by immersing them individually into the DMSO-d_6 and POSS-CT was immersed in $CDCl_3$ then do the ultrasonication for 30 minutes to dissolve the substance into d-solvent.

3.5.3 X-ray Photoelectron Spectroscopy (XPS)

The X-ray photoelectron spectroscopy (XPS) analysis of samples were measured by X-ray Photoelectron Spectroscopy (ThermoFisher Scientific, Waltham, MA, ISA) with Argon to clean up the surface for 5 s before analysis.

3.5.4 Field-emission Scanning Electron Microscope (FE-SEM)

The FE-SEM images were obtained using Nova NanoSEM 230 (ThermoFisher Scientific, Waltham, MA, USA) The samples were dried at 40℃ in vacuum overnight before FE-SEM measurement.

doi:10.6342/NTU202101615

3.5.5 Static Contact angle measurement

The static contact angles of samples were measured by Contact Angle System (FTA125). 5 μL of water or diiodomethane droplet was dipped onto the sample surface for contact angle measurement.

3.5.6 Ultraviolet-visible spectroscopy (UV-vis)

The UV-vis spectra was measured by UV/VIS Spectrophotometer Cary 300 (Varian, Midland, Canada) from wavelength 800 nm to 200 nm. The floating hexane were mixed well then do the UV-vis measurement to evaluate the content of hexane.

3.5.7 Absorption capacity

The absorption capacity was evaluated by measuring the weight of absorbed liquid divided by the weight of fabric. The equation was shown in the following

$$\textbf{Absorption capacity} = \frac{\boldsymbol{Weight\ gain\ of\ absorbed\ fabric - Weight\ of\ original\ fabric}}{\boldsymbol{Weight\ of\ fabric}}$$

3.5.8 Oil absorption capacity

The absorption test is shown in Figure 3-3 (a) Test I with fabric is placed horizontally to hexane layer floating on 5 cm water layer for 30 s. (b) Test II for the cotton fabric composing of step I with fabric immersed horizontally into 5 cm water for 30 s then the fabric is immersed horizontally into another 5 cm hexane layer for another 30 s.

doi:10.6342/NTU202101615

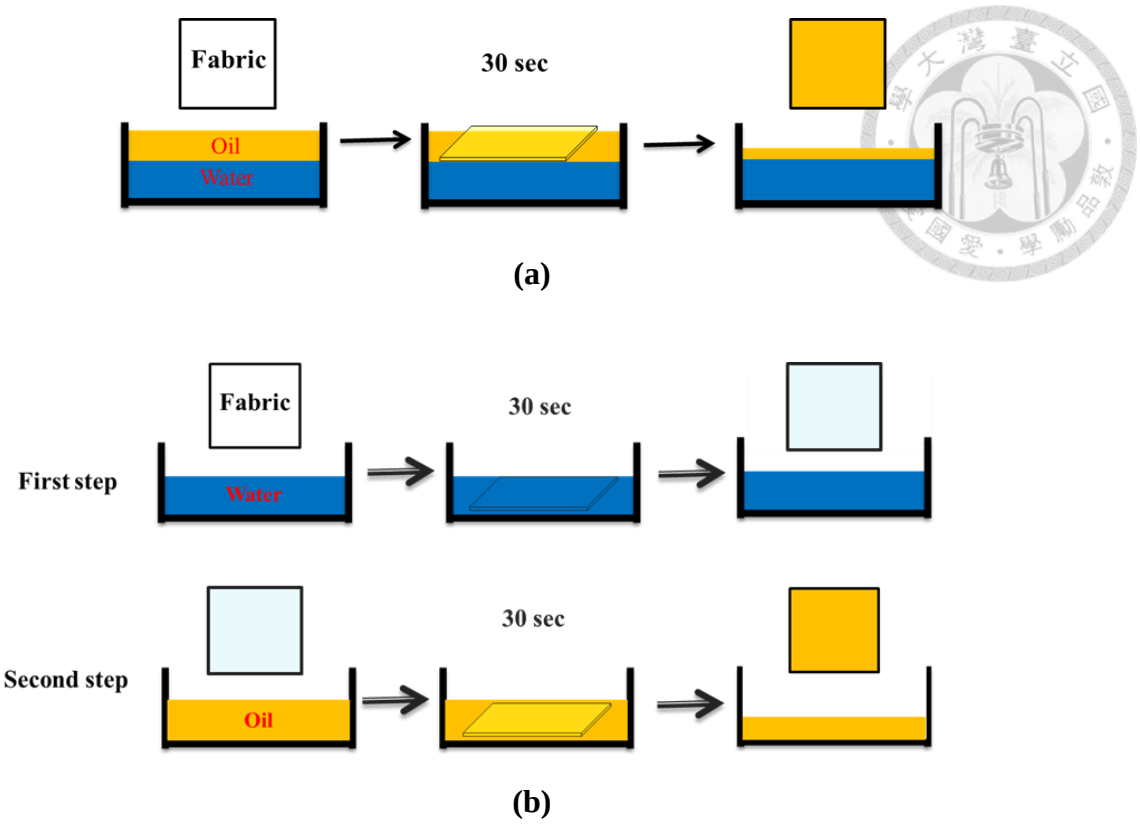

Figure 3-3. The absorption test (a) Test I (b) Test II

doi:10.6342/NTU202101615

Chapter 4
Result and Discussion

4.1. POSS-modified cotton fabric

4.1.1 The functional groups of cotton fabric, SH-CT and POSS-CT

Figure 4-1 shows the FTIR spectra of the cotton fabric samples. The broad FTIR peaks of pristine cotton fabric around 3450 cm^{-1}, and the peaks at 2902 and 1704 cm^{-1} correspond to -OH stretching, CH_2 stretching [59,69], and C=O stretching vibration [27], respectively. After modification, the peak of –SH group for SH-CT was not significant owing to the limited content of MPTES [146, 164]. After modification of POSS, the peak at 1111 cm^{-1} and 790 cm^{-1} were reinforced because of the stretching vibration of Si-O linkage [146, 165] and stretching vibration of Si-C [20, 165], attributed to the presence of POSS.

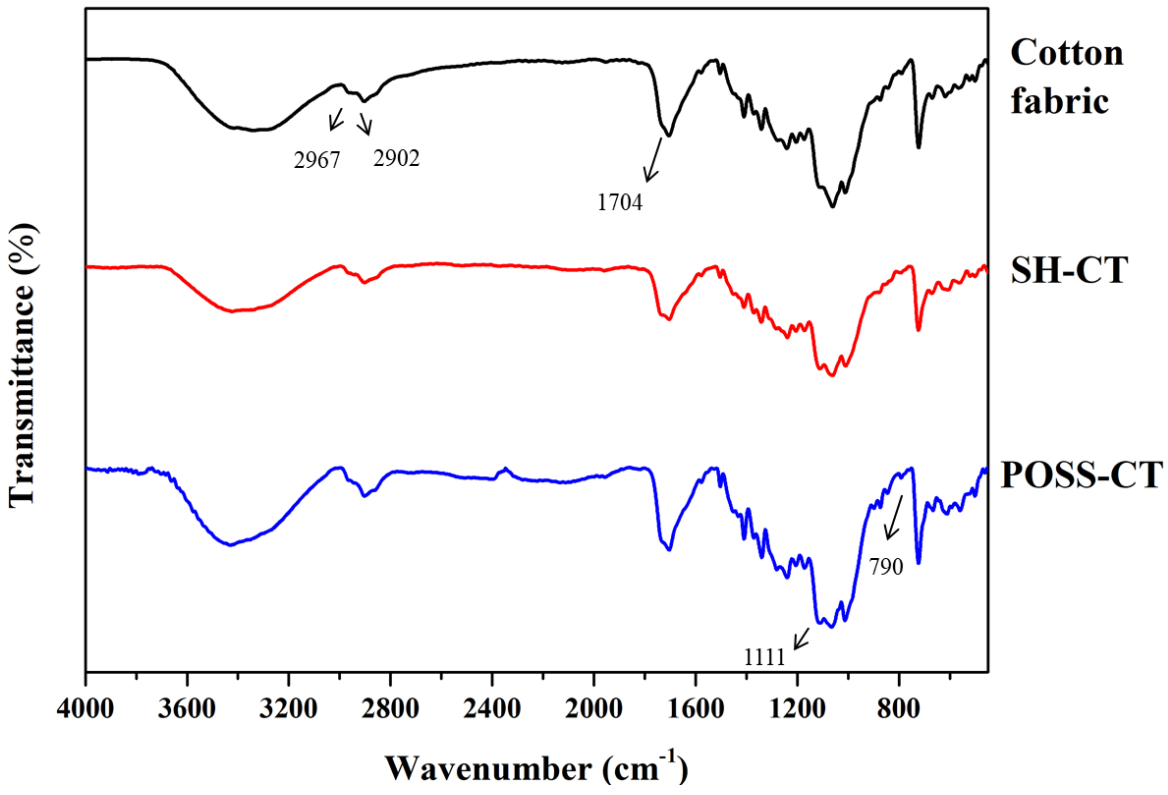

Figure 4-1. The FTIR spectra of cotton fabric, SH-CT and POSS-CT

doi:10.6342/NTU202101615

4.1.2 The structure of POSS, MPTES and POSS-CT

Figure 4-2 shows the ^{1}H NMR spectra of the POSS, MPTES and POSS-CT. The signals of 5.87-6.10 ppm is assigned to the vinyl group of POSS [166, 167]. The signals at 1.26 and 1.14 ppm are contributed by the thiol group and -CH_2 of MPTES [168]. After the POSS is anchored on the MPTES, the signals for vinyl groups of POSS is observed at 8.87-6.10 ppm. Furthermore, the new signals appeared at 2.0-2.3 ppm ascribing to the occurrence of the thiol-ene click reaction [147].

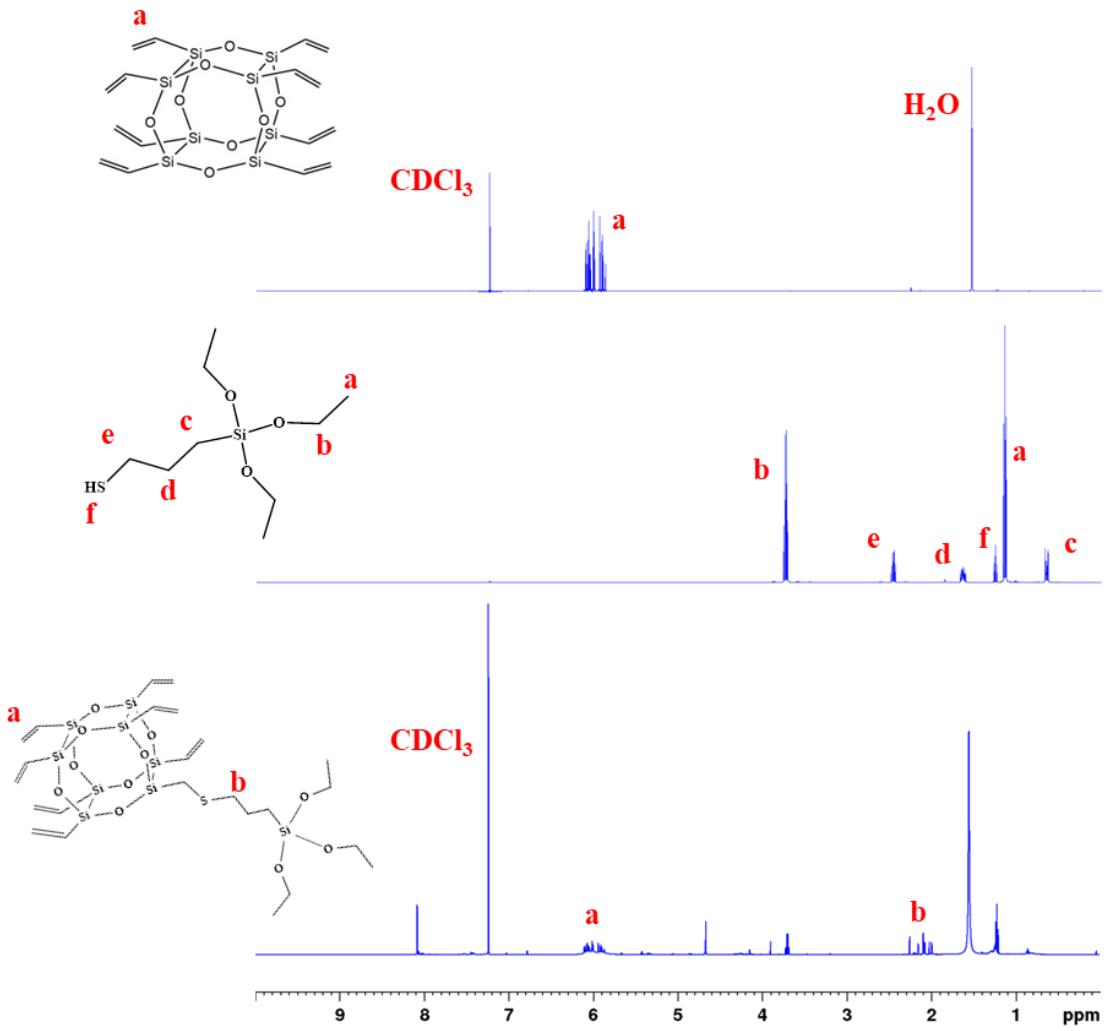

Figure 4-2. The ^{1}H NMR spectra of POSS, MPTES and POSS-CT

doi:10.6342/NTU202101615

4.1.3 The binding energy of cotton fabric, SH-CT and POSS-CT

Figure 4-3a shows the XPS spectra of the cotton fabrics samples. With MPTES anchored on the cotton surface, the peaks of S_{2s}, $S_{2p,}$ Si_{2s} and Si_{2p} are detected in the spectra for SH-CT. After SH-CT is further incorporated with POSS, the intensities of Si_{2s} and Si_{2p} are reinforced which proves the cotton fabric is successfully modified.

As shown in Fig. 4-3b, the peak for C-Si bond is ascribed to the linkage of POSS [169]. The peak of C-O/C-S and C=O are detected at 286.4 eV and 288 eV, respectively. The peak at 288.6 eV of C=C is attributed to the vinyl structure of POSS that represent POSS is significantly anchored on the fabric [20]. Table 4 lists the areal fractions of C_{1s} peaks.

doi:10.6342/NTU202101615

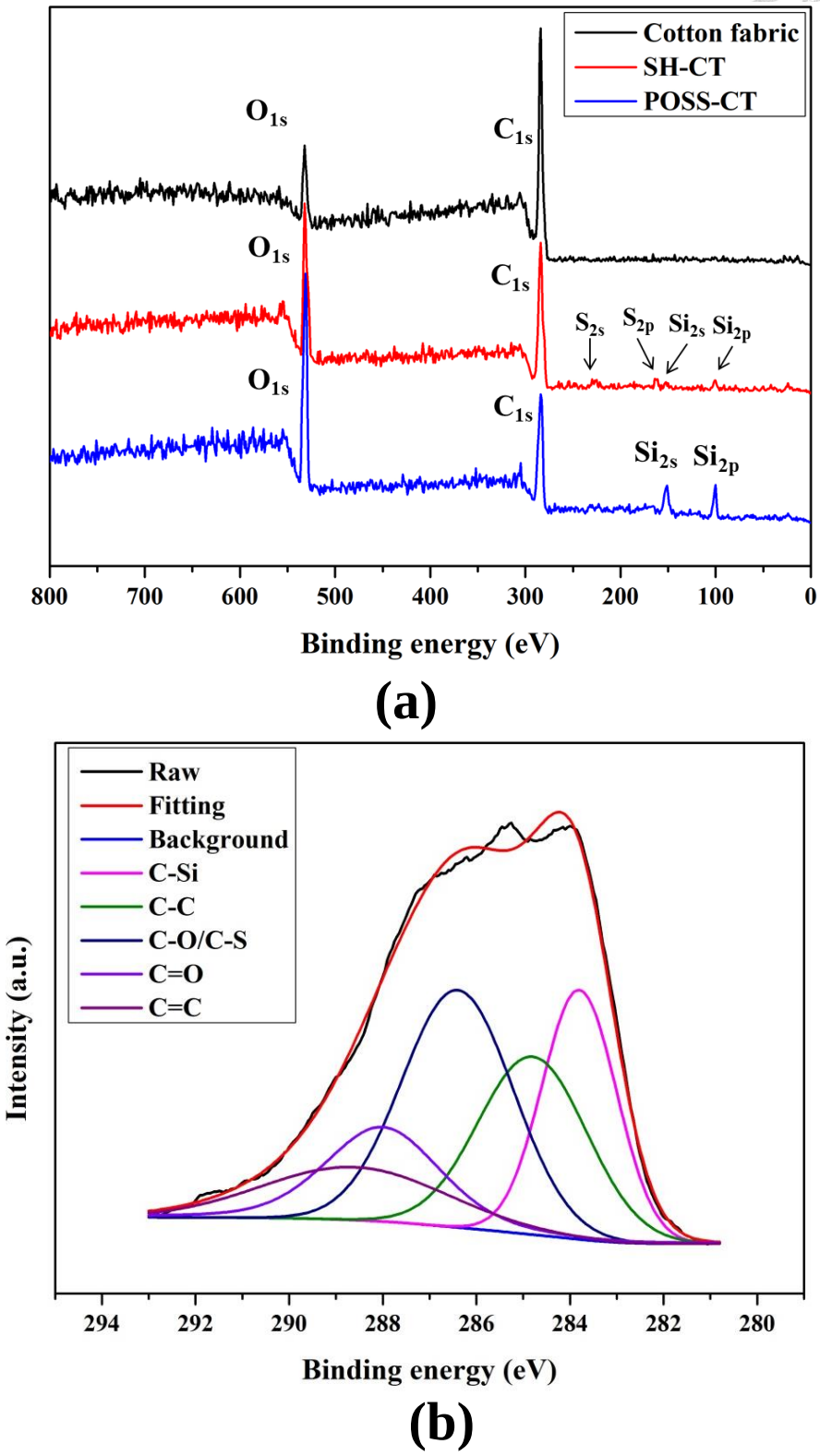

Figure 4-3. The XPS spectra of POSS-CT. (a) wide scanning; (b) binding energy for C_{1s}

doi:10.6342/NTU202101615

4.1.4 The morphology of surface for cotton fabric, SH-CT and POSS-CT

Figure 4-4 shows the SEM images of cotton fabric, SH-CT and POSS-CT. Small particles are deposited on the fabric surface after being coordinated with MPTES (Fig. 4-4b). After MPTES modification, 1.06% w/w silicon and 1.53% w/w sulfur are detected on the fabric, corresponding to the thiol-containing silane (Fig. 4-4e).

Rough surfaces were noted for parts of the POSS-CT surface (Fig. 4-4c). The EDS spectra of POSS-CT shows enriched silicon to 6.39% w/w owing to presence of POSS (Fig. 4-4f).

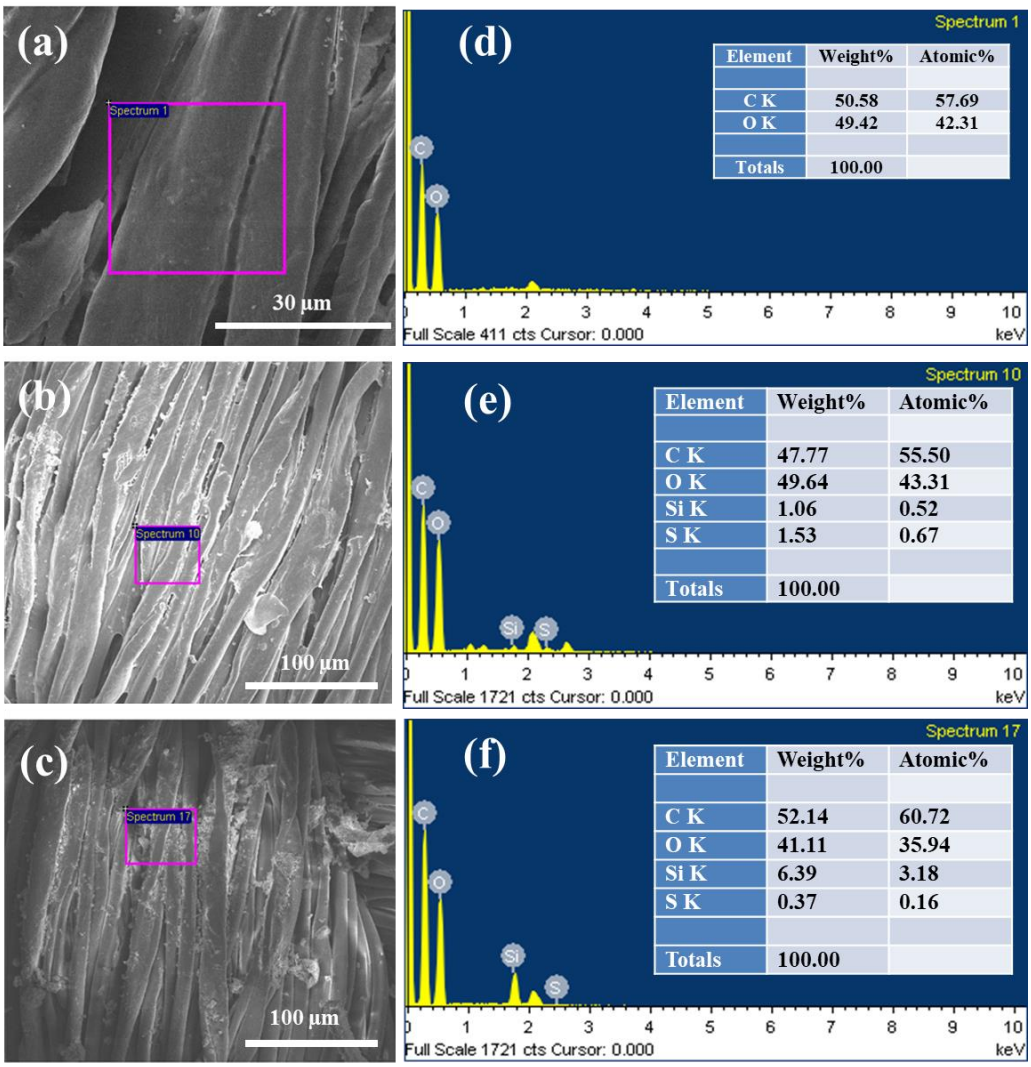

Figure 4-4. FE-SEM images (a-c) and EDS spectra (d-f) of cotton fabrics. (a, d) cotton fabric; (b, e) SH-CT; (c, f) POSS-CT

doi:10.6342/NTU202101615

4.1.5 Contact angle measurements

Table 4 shows the contact angles for water and diiodomethane droplets on the POSS-CT fabric surface, for the former being 142.82±1.17° and the latter, 0°. Restated, the POSS-CT is highly hydrophobic in nature and has high affinity to alkyl groups. The components of surface energy of a smooth surface could be described by the equation (4). The terms with superscripts p denote that they are polar components, and those with d denote that they are dispersive components of the surface energy. Based on eq. (4), the polar component and dispersive component of surface energy were estimated as 13.1 mJ/m^2 and 50.8 mJ/m^2, giving total surface energy of 63.9 mJ/m^2 as listed in Table 4. Based on estimated polar component and dispersive component and eq. (4), the wetting envelope can be depicted (Fig. 4-5). The liquid with components locating outside the envelope cannot wet the solid surface with the wetting envelope. Based on Fig. 4-5, the POSS-CT can not be wet by water droplet but can be wet by common oil products. Conversely, the PTFE cannot be wet by either water or oil droplet.

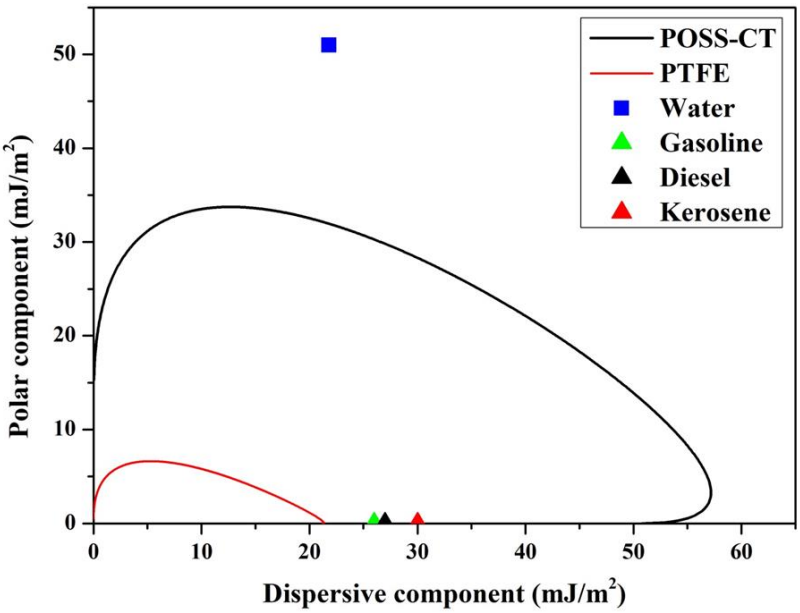

Figure 4-5. The wetting envelope of POSS-CT, PTFE, and those for water, gasoline, diesel, and kerosene

doi:10.6342/NTU202101615

4.1.6 Water contact angle for POSS-CT

Figure 4-6 shows the effects of reaction parameters on the water contact angle on the POSS-CT surface. For POSS reacted with SH-CT for 1 hr, the water contact angle would increase with concentration of POSS, maximizes to 142.82±1.17° at 1.6% w/w, then slowly declines when POSS concentration is increased further. The impact of POSS concentration on water contact angle is mild.

With 1.6% w/w POSS concentration, the reaction time increases the water contact angle, reaching 143.28±0.40° with reaction time of 70 min. It is noticeable that the increase in water contact angle for reaction time is increased from 60 to 70 min is not significant.

As Fig.4-6 shows, the water contact angle would decrease when the contact time is increased, reducing to 138.20±0.83° after nine min contact time. This observation suggests that certain deterioration of surface hydrophobicity occurs on POSS-CT surface, which may be attributable to fiber swelling for absorbing certain quantity of water, relaxation of polymer chains to water invasion, or POSS detachment from the surface. Nonetheless, the POSS-CT remains highly hydrophobic over the testing period for oil/water separation.

doi:10.6342/NTU202101615

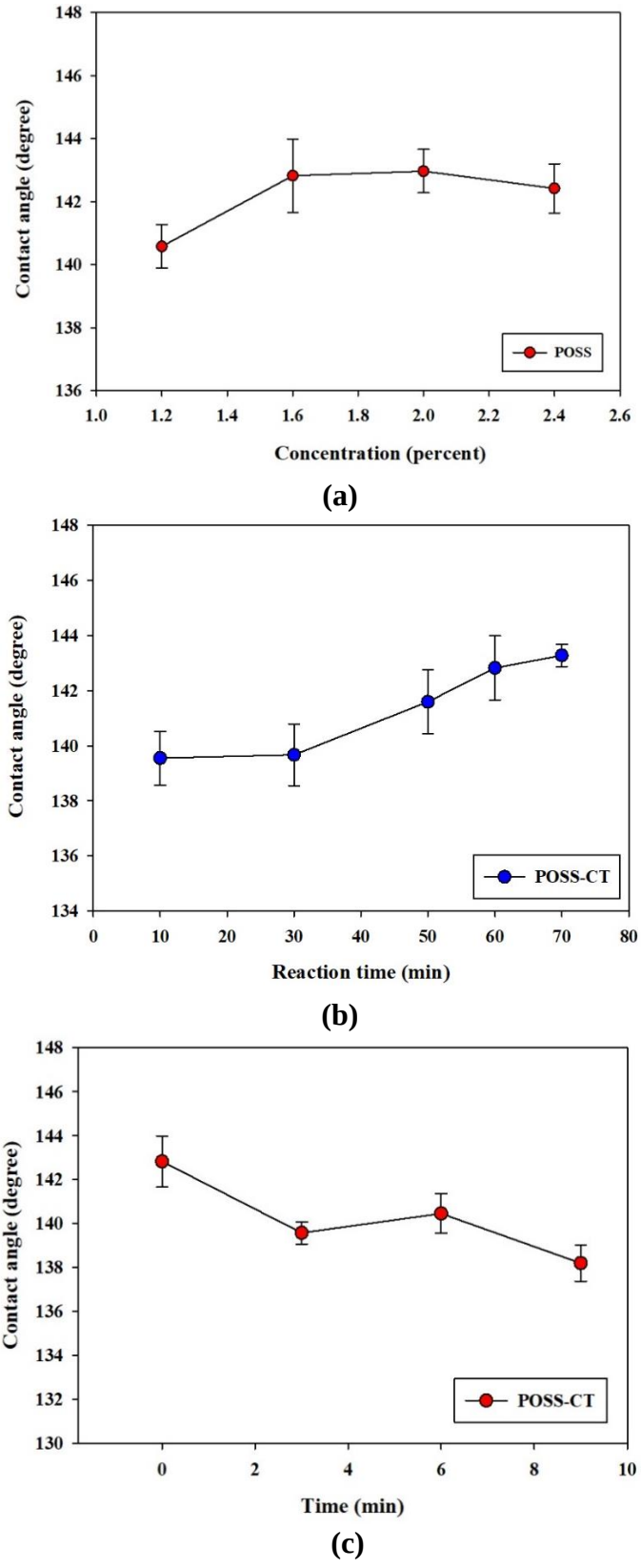

Figure 4-6. Effects of reaction parameters on water contact angles for POSS-CT. (a) Effects of POSS concentration on water contact angles for 1 hr reaction time; (b) effects of reaction time to water contact angle with 1.6% w/w POSS concentration; (c) effects of contact time on water contact angle. POSS-CT modified by 1.6% w/w POSS for 1 hr.

doi:10.6342/NTU202101615

4.1.7. Oil absorption capacity

The results of test I shown in Table 4 revealed that POSS-CT adsorbed 0.17 g/g water and 0.96 g/g hexane when immersed into the water+oil layers. The POSS-CT can adsorb more oil than water when contacting these two fluids simultaneously. This observation correlates with the hydrophobic characteristics of the POSS-CT surfaces noted in Sec. 4.1.5.

The results of test II are also listed in Table 4. When the POSS-CT contacts water layer first, it can absorb 0.86 g/g water, much higher that for test I. When the water-absorbed POSS-CT contacts the hexane layer, it can absorb 1.12 g/g hexane, about 16.7% higher than that in Test I. The POSS-CT can intake water by its main pores while possesses remaining pore space to accommodate sufficiently high capacity for hexane. The POSS-CT is an efficient absorbent for oil/water separation from oil-water mix.

doi:10.6342/NTU202101615

Table 4. Measurement results and calculations for POSS-CT fabrics

XPS C_{1s} spectra					
Bond	C-Si	C-C	C-O/C-S	C=O	C=C
Binding energy (eV)	283.8	284.8	286.4	288.0	288.6
Area	338.3	351.6	479.0	222.1	177.2
Areal fraction (%)	21.6	22.4	30.5	14.2	11.3

Contact angle measurement		
	Image	Contact angle
Water	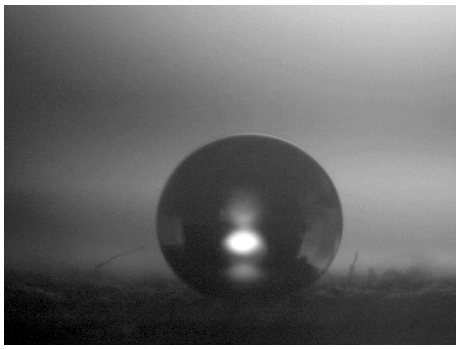	142.82±1.17°
Diiodomethane		0°

Estimation of surface energy		
Polar component	Dispersive component	Surface energy
13.13±0.13 mJ/m^2	50.8±0.02 mJ/m^2	63.93±0.13 mJ/m^2

The absorption capacity of fabric for water and hexane in Test I and Test II.	
Test I	
Absorption capacity (g water/g cotton)	Absorption capacity (g hexane/g cotton)
0.17±0.02	0.96±0.03
Test II	
Absorption capacity (g water/g cotton)	Absorption capacity (g hexane/g cotton)
0.86±0.12	1.12±0.04

doi:10.6342/NTU202101615

4.2 Tannic acid-modified cotton fabrics

4.2.1 The functional groups of cotton fabric and tannic acid-modified cotton fabrics

After modification, the intensities of 2967 and 2902 cm^{-1} peaks were increased contributed by the long alkyl chains of ODA, HDA and TDA [28]. The broadened peaks of -OH stretching (around 3350 cm^{-1}) and C=O stretching vibration (1704 cm^{-1}) are ascribed to the catechol structures and quinone groups of tannic acid [173]. The intensity of peak intensity at 1505 cm^{-1} is increased by the added of -CN for the modified cotton fabrics [28]. The formation of -C=N leads to 1637 cm^{-1} in the result of Schiff base reaction [69].

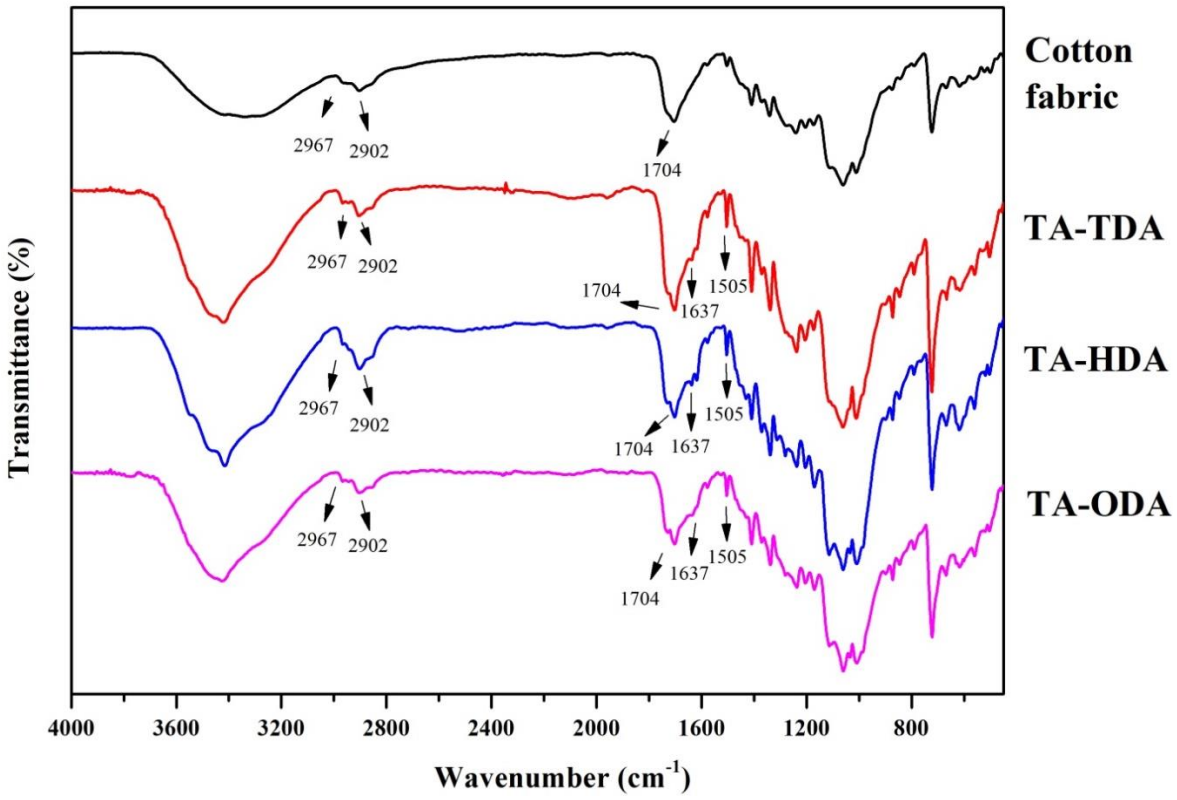

Figure 4-7. The FTIR spectra of cotton fabric, TA-TDA, TA-HDA, TA-ODA

doi:10.6342/NTU202101615

4.2.2 The structure of tannic acid, long chain alkyl amine and tannic acid-modified cotton fabrics

Figure 4-9 shows the ^{1}H NMR spectra of the tannic acid-alkylamine coatings samples. The signal at 1.22 ppm corresponds to the long chain alkyl groups of TDA, HDA and ODA [174,175]. The signals at 9.5-9 ppm and 7.5-6.7 ppm are ascribed to the phenolic hydroxyls and aromatic proton of tannic acid, respectively [176,177]. After reaction between tannic acid and alkylamines, new signals appear at 1.43 and 3.24 ppm, which represent the consequence of Schiff base reaction [30, 174] and Michael addition reaction [176, 178] respectively. The peak at 1.22 ppm remains unchanged after reaction, representing the tannic acid-based coating that consist of the long chain alkyl structure. The ^{1}H NMR spectra of the modified cotton fabric support the successful modification of cotton surface with tannic acid-alkylamine coatings.

doi:10.6342/NTU202101615

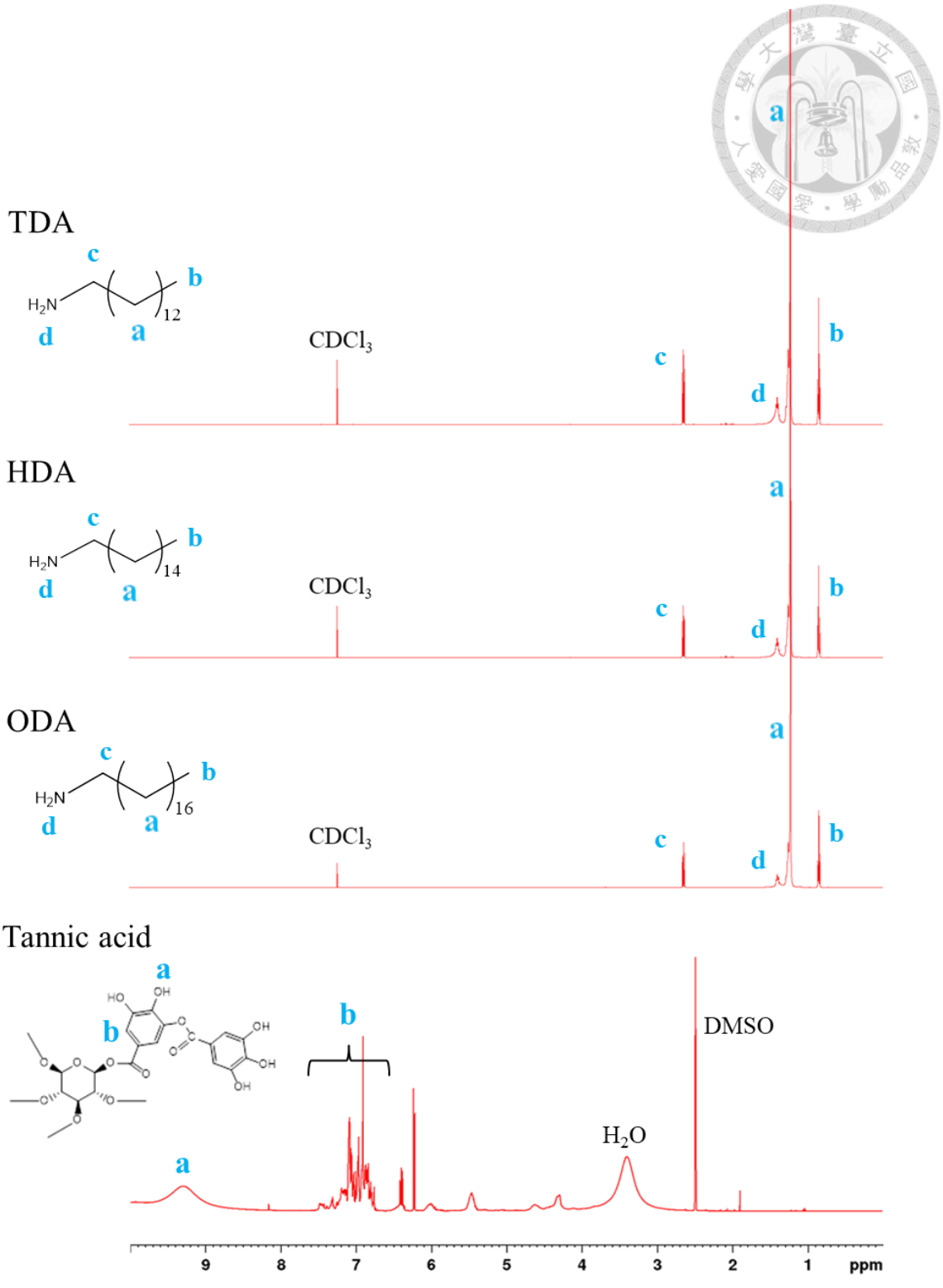

Figure 4-8. The ^{1}H NMR spectra of TDA, HDA, ODA and tannic acid

doi:10.6342/NTU202101615

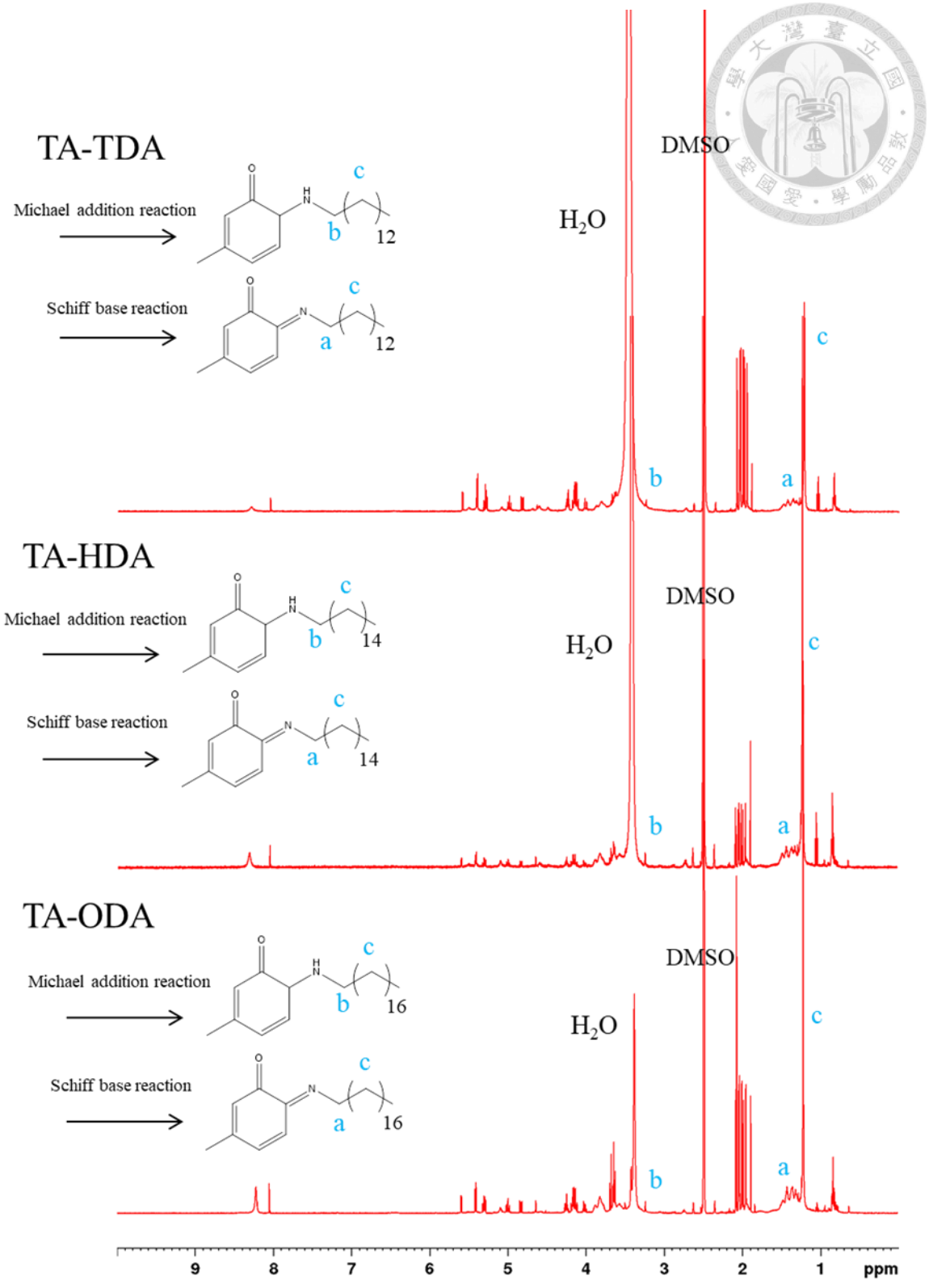

Figure 4-9. The ^{1}H NMR spectra of TA-TDA, TA-HDA and TA-ODA

doi:10.6342/NTU202101615

4.2.3 The binding energy of cotton fabric, TA-TDA, TA-HDA and TA-ODA

Figure 4-10 shows the XPS spectra of the cotton fabrics samples with the areal fractions of C_{1s} peaks listed in Table 5. The pristine cotton surface has C_{1s} peaks at 284.8 eV, 286.3 eV, and 288.3 eV, corresponding to C-C, C-O and C=O bonds, respectively, with the former two being the major bonds for C atoms [22, 23]. With TA-TDA, TA-HDA and TA-ODA coatings, the surface of cotton surface has excess C-O and C=O bonds, characteristics of TA [173, 179]. The enriched -C=N and C-N bonds signal the presence of amide groups in the modified surfaces. The areal ratio for C-C is increasing with increased chain length of the alkyl groups, suggesting that the increased contribution of Michael addition reaction and the Schiff base reactions with longer alkylamines with TA (Table 5).

doi:10.6342/NTU202101615

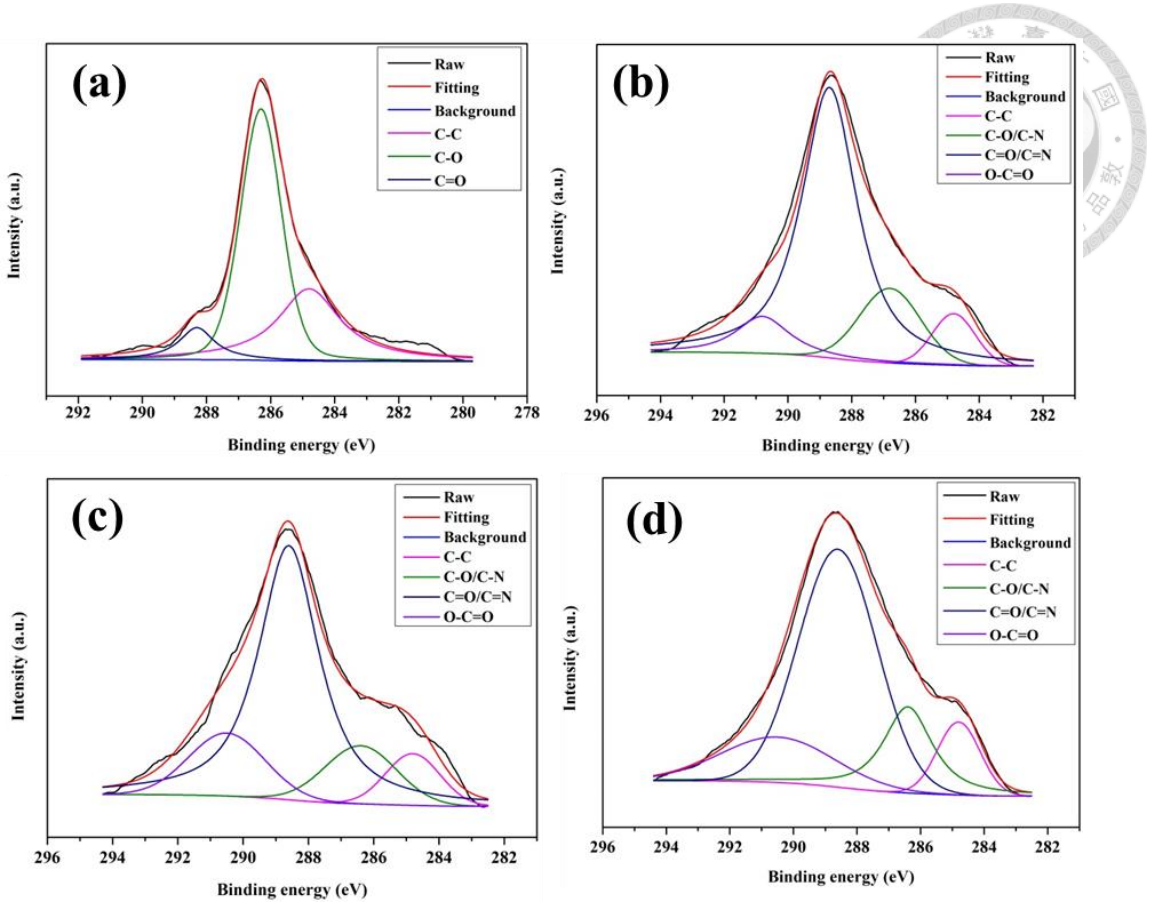

Figure 4-10. The XPS spectra of C_{1s} for cotton fabric (a), TA-TDA (b), TA-HDA (c) and TA-ODA (d)

Table 5. The binding energy value of C_{1s} for pristine and modified cotton fabrics

		C-C	C-O	C=O	
Pristine cotton	Binding energy (eV)	284.8	286.3	288.3	
	area	894.0	1344.5	223.8	
	Area fraction (%)	36.3	54.6	9.1	
		C-C	C-O/C-N	C=O/C=N	O-C=O
TA-ODA fabric	Binding energy (eV)	284.8	286.4	288.6	290.5
	area	104.6	262.7.5	844.1	232.2
	Area fraction (%)	9.5	17.7	57.1	15.7
		C-C	C-O/C-N	C=O/C=N	O-C=O
TA-HDA fabric	Binding energy (eV)	284.8	286.4	288.6	290.5
	area	127.6	189.4	971.3	217.5
	Area fraction (%)	8.5	12.6	64.5	14.4
		C-C	C-O/C-N	C=O/C=N	O-C=O
TA-TDA fabric	Binding energy (eV)	284.8	286.4	288.6	290.5
	area	104.7	216.5	991.1	128.2
	Area fraction (%)	7.3	15.0	68.8	8.9

doi:10.6342/NTU202101615

4.2.4 The morphology of surface for fabrics

The surfaces of pristine cotton fabric appear smooth (Figure 4-11a), while the surface possessed mainly C and O atoms as characterized by EDS (Figure 4-11e). The surfaces of TA-TDA, TA-HDA and TA-ODA modified cotton fabrics with catalysts 5 mM $CuSO_4$ and 19.6 mM H_2O_2 and reaction time 60 min are roughened (Figures 4-11b-d). As Figures 4-11f-h show, the cotton fabrics have incorporated N atoms, suggesting the appearance of amide groups on the modified surface.

doi:10.6342/NTU202101615

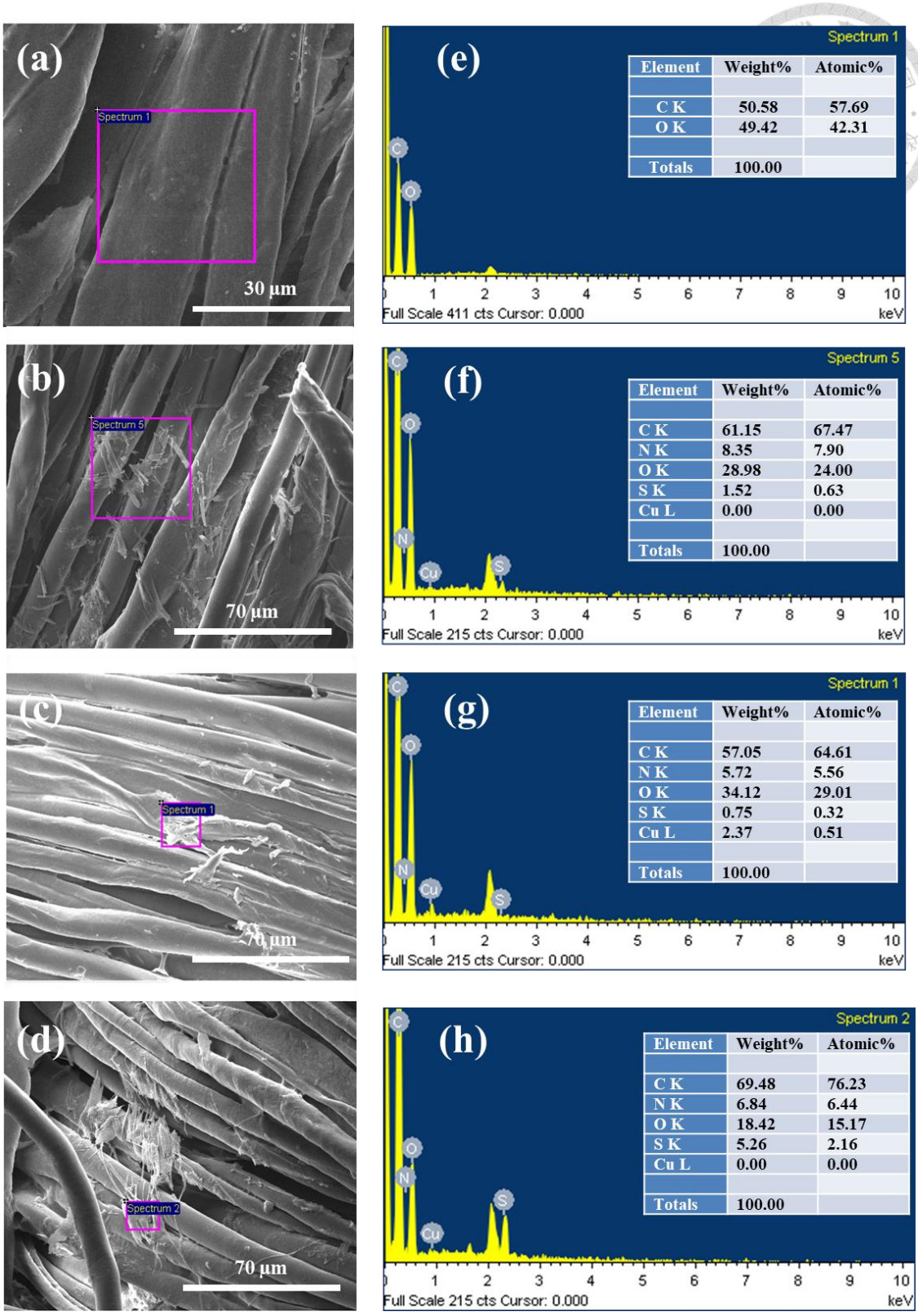

Figure 4-11. FE-SEM images (a-d) and EDS spectra (e-h) of cotton fabrics. (a,e) Pristine; (b,f) TA-TDA; (c,g) TA-HDA; (d,h) TA-ODA.

doi:10.6342/NTU202101615

4.2.5 Contact angle measurements

Table 6 shows the static contact angles for droplets of water or diiodomethane on the cotton fabric surfaces with catalysts 5 mM $CuSO_4$ and 19.6 mM H_2O_2 and reaction time 60 min. The contact angles of water droplets on pristine cotton fabrics is close to zero, correlating with the hydrophilic surface composed of cellulose. After modification, the contact angles for water droplets on the modified surface are 133.3^o, 136.0^o and 142.9^o for TA-TDA, TA-HDA, and TA-ODA cotton fabrics, respectively. Restated, all modified surfaces are hydrophobic that reject water. The corresponding contact angles for diiodomethane droplets are 56.0^o, 58.8^o and 59.3^o, respectively. Restated, these surfaces are affine to oil compounds. Overall, the modified surfaces have contact angles of water larger than PFTE, and lower contact angles of diiodomethane droplet than PTFE (Table 6).

Table 6 also lists the calculated surface energies for the modified cotton fabrics. The surface energies of the modified surfaces have very low polar component (4.2-6.2 mJ/m^2) and intermediate dispersive component (29.0-31.2 mJ/m^2). Restated, these surfaces should have low affinity to water and intermediate attraction to hydrophobic compound. Compared with PTFE, the current modified surfaces have higher polar components and dispersive components.

The three modified surfaces are grafting with TA and long chain alkylamines, with TA-TDA, TA-HDA and TA-ODA differing with two methyl groups each (14, 16, and 18, respectively). The increase in every two methyl groups, though with limited magnitudes, is noted to increase the polar component but decrease the dispersive component of surface energies. This observation contradicts to the interpretations that longer alkyl chain length would lead to higher dispersive component and lower polar component. Such an observation may be owing to the possible packing of alkyl groups in the grafted layer so their volume is reduced, yielding reduced dispersive component. The more aligned alkyl top layer can yield more aligned bottom TA molecules on surface, which would possibly lead to more polar interactions such as hydrogen bonding between TA molecules, so generating increased polar component. Regardless of the interpretation, the increase or decrease in components are limited.

doi:10.6342/NTU202101615

Based on figure 4-12, the modified cotton fabrics can be wet by common oil compounds but not by water. Therefore, the modified surfaces have been properly designed and synthesized so they can be used as adsorbents for spilled oil from water-oil mix.

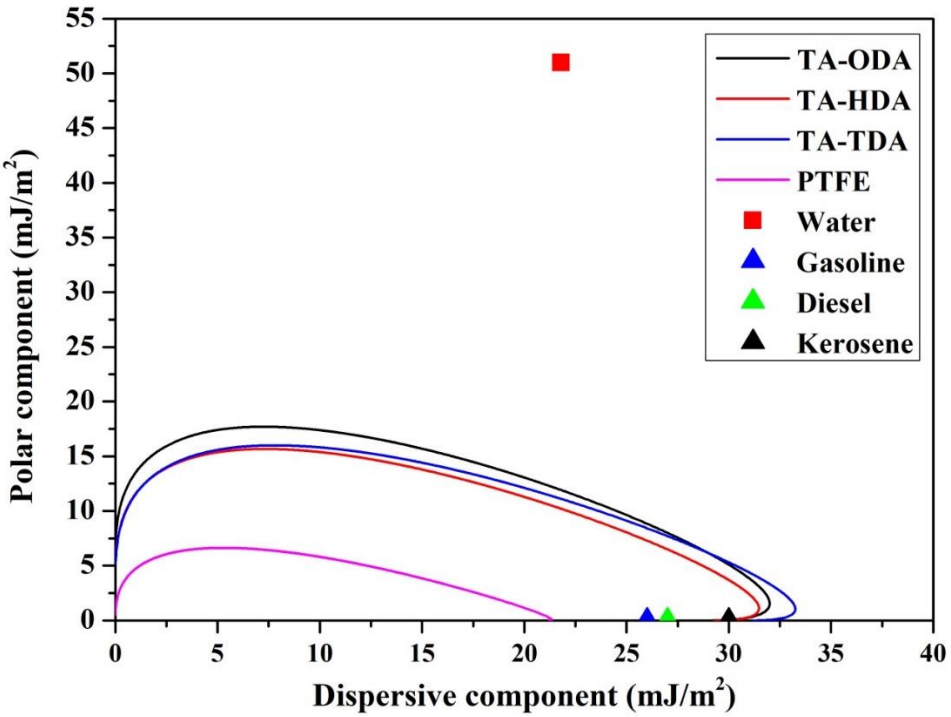

Figure 4-12. The wetting envelope of TA-ODA, TA-HDA and TA-TDA cotton fabrics, PTFE, and those for water, gasoline, diesel, and kerosene

doi:10.6342/NTU202101615

Table 6. The contact angles of modified cotton fabrics with water and diiodomethane droplets.

	Water (degree)	Image	Diiodomethane (degree)	Image	Dispersive component (mJ/m^2)	Polar component (mJ/m^2)
TA-TDA	133.27±1.15		56.01±5.11	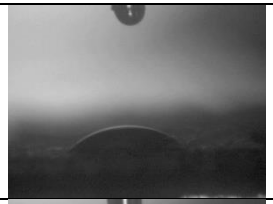	31.2	4.2
TA-HDA	135.99±1.15		58.75±4.13		29.3	4.4
TA-ODA	142.87±0.53		59.30±4.10		29.0	6.2
PTFE*	108.0±1.5	NA	73.0±3.2	NA	21.2	0.27

* Data from Milne and Ritchie (2007) and Al-Maliki (2018).

doi:10.6342/NTU202101615

4.2.6 Anti-wetting ability

Figure 4-13 demonstrates the anti-wetting ability of TA-ODA, TA-HDA and TA-TDA cotton fabrics farbicated with 60 minutes of reaction time. TA-ODA and TA-HDA remain high contact angle after ten minutes which show excellent water resistance. The great water repellency is attributed to hydorphobicity property of long chain hydrocarbon compound grafted on the surface . Compared to TA-HDA, TA-TDA shows poor water resistance because of the shorter chain length of alkyamine.

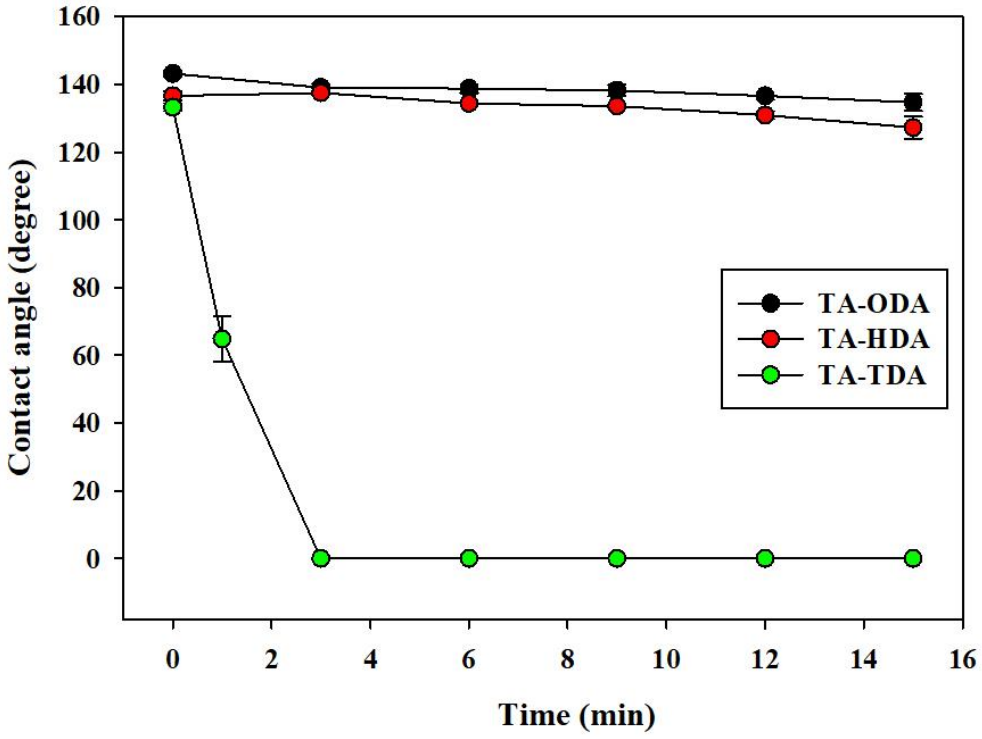

Figure 4-13. The wetting resistance of TA-ODA, TA-HDA and TA-TDA

doi:10.6342/NTU202101615

4.2.7 Effects of reaction parameters for alkylamine grafting

To observe whether the adopted catalysts are needful for reaching satisfactory modification of cotton fabrics, Figure 4-14 shows the reaction parameters on the measured contact angle using water droplets. The reaction time of 10-70 min for TA-TDA, TA-HDA, TA-ODA cotton fabrics at 5 mM $CuSO_4$, 19.6 mM H_2O_2 at pH 8.5 has mild effects on contact angles of water droplets on these modified cotton fabrics (Fig. 4-14a). For instance, the contact angle of water droplets on TA-ODA, TA-HDA and TA-TDA cotton fabrics are 139.67±1.07°, 133.05±1.54° and 130.77±1.65° for 10 min reaction, and are increased to 142.87±0.53°, 135.99±1.15° and 133.27±1.15° respectively at 60 min reaction.

Figure 4-14b shows the reaction of 10-70 min for TA-ODA, TA-HDA and TA-TDA with no $CuSO_4/H_2O_2$ at pH 8.5. The contact angle of water droplet on TA-ODA, TA-HDA, TA-TDA are 134.19°±1.12°, 132.06°±1.02° and 128.74°±1.25° for 10 min reaction. As the reaction time is increased to 60 min, the contact angle of TA-ODA, TA-HDA and TA-TDA are enhanced to 135.29°±1.49°, 133.65°±0.88° and 129.55°±1.13°. The contact angle of TA-HDA increases more obviously during 0-30 min reaction time.

Figure 4-14c shows the effects of H_2O_2 concentration with 0 mM $CuSO_4$ at pH 8.5 for TA-ODA cotton fabrics. As reaction time exceeds 30 min, the contact angles of water droplet on TA-ODA cotton fabric surface reaches a plateau, whole value is increasing with concentration of H_2O_2.

Figure- 4-14d shows the effects of $CuSO_4$ concentration with 19.6 mM H_2O_2 at pH 8.5 for TA-ODA cotton fabrics. The contact angle of water droplets on TA-ODA cotton fabric surface increases with increasing reaction time, with the increasing trend more obvious during 0-30 min reaction time for modification without $CuSO_4$ than those with 5 or 10 mM $CuSO_4$.

Figure 4-14e shows the effects of pH values with 5 mM $CuSO_4$ and 19.6 mM H_2O_2 for TA-ODA cotton fabrics. The contact angle of water droplets on TA-ODA cotton fabric surface increases with increasing reaction time and reach plateau at > 30 min reaction time. At the same reaction time, the contact angle of water droplet on

doi:10.6342/NTU202101615

TA-ODA cotton fabric surface is increasing as pH is raised from 5.5, maximizing at pH 8.5, and then declines as pH is increased further to 9.5.

The above tests reveal that the currently adopted recipe with catalyst 5 mM $CuSO_4$/19.6 mM H_2O_2 is appropriate for modification of the TA-ODA cotton fabrics. The reaction time can be reduced to 10 min if the pH value can be maintained at 8.5 to enhance formation rate of quinones groups for crosslinking reaction, which is adjusted in this work by Tris base and HCl. Therefore, the tests with no $CuSO_4$ or H_2O_2 addition, or using inexpensive base for pH adjustment can indicate the potentials to reduction of chemical costs; conversely, the reaction time acquired may increase to reach satisfactorily high contact angles that would increase the operation cost. Further studies are needed to find the optimal modification coditions with satisfactory performance for oil/water separation at minimum total costs.

doi:10.6342/NTU202101615

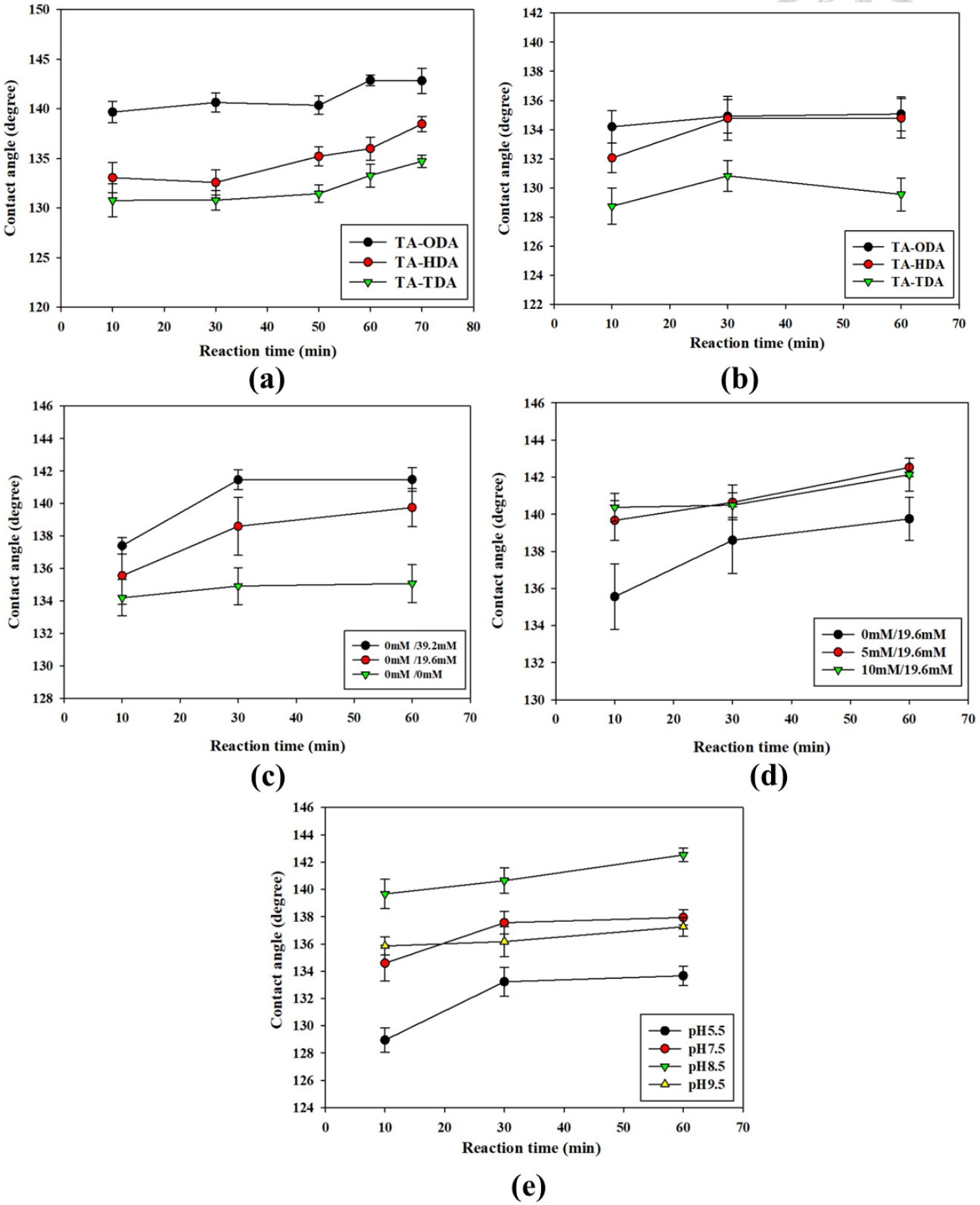

Figure 4-14. Effects of reaction parameters on contact angles water droplets on the modified cotton fabrics. (a) 5 mM $CuSO_4$, 19.6 mM H_2O_2, pH 8.5; (b) no $CuSO_4$, no H_2O_2, pH 8.5 (c) TA-ODA, no $CuSO_4$, pH 8.5; (d) TA-ODA, 19.6mM H_2O_2, pH 8.5; (e) TA-ODA, 5 mM $CuSO_4$, 19.6 mM H_2O_2

doi:10.6342/NTU202101615

4.2.8 Oil absorption capacity

As Lin and Lee [15] commented, the testing protocols commonly applied in cotton absorbent literature for oil absorption capability from water-oil mix need revision. We adopted two different tests herein to simulate the scenario in field applications. When an oil compound is poured into a water pool, it can float [8] or sink [170] depending on its relative density to water. The pool tests applied in literature with passing a water layer with one or two immiscible oil layers to over the cotton fabric should be able to reveal the affinity of the cotton fabric to oil than water [19]. However, since the two liquids are immiscible the first liquid, water or oil, that contacts the fabric tends to block the main internal pores of fabrics to hinder subsequent flow of another immiscible liquid, the validity of the pool test is questioned [15].

The test I results are shown in Table 7. The pristine cotton fabric can adsorb 0.87 g/g water and 0.35 g/g hexane when immersed into water+oil layers. Restated, the hydrophilic cotton can adsorb finite quantity of oil when contacting water-oil layers, which should be accomplished by the entrance of main pores by oil regardless of the surface hydrophobicity. For the modified cotton fabrics, the quantities of water absorbed are decreased to around zero while those of hexane are increased to 0.96-1.01 g/g. The hydrophobic surfaces of modified fabrics would have high affinity to oil and decline the intake of water to the fabrics.

The test II results are also shown in Table 7. For TA-TDA, TA-HDA and TA-ODA cotton fabrics with 5mM/19.6mM of $CuSO_4/H_2O_2$ for 60 min of reaction time, they can adsorb less water (1.15-1.80 g/g) and absorb more hexane (0.52-0.97 g/g) in the second stage of test compared to pristine cotton fabrics shown in Table 7.

Table 8 shows the water and oil absorption capacity for modified fabrics with 5mM/19.6mM of $CuSO_4/H_2O_2$ for 10 min of reaction time. They are enable to absorb

doi:10.6342/NTU202101615

water (1.16-1.90 g/g) and hexane (0.57-1.07 g/g) exhibiting great oil absorption as well as the modified fabrics with 60 min of reaction time.

Table 9 shows the the water and oil absorption capacity for modified fabrics with no $CuSO_4/H_2O_2$ for 10 min of reaction time. The modified fabrics are able to absorb (1.07-1.94 g/g) water and (0.44-0.1.04 g/g) hexane. Without adding $CuSO_4/H_2O_2$ for fabrication, the modified fabrics shows great oil absorption capability as well as the modified fabric with $CuSO_4/H_2O_2$ shown in Table 8.

doi:10.6342/NTU202101615

Table 7. The absorption capacity of fabrics for water and hexane in Test I and Test II.

Test I		
	Absorption capacity (g water/g cotton)	Absorption capacity (g hexane/g cotton)
Cotton	0.87±0.27	0.35±0.26
TA-TDA	0.17±0.15	0.96±0.14
TA-HDA	0.18±0.15	1.00±0.10
TA-ODA	0.14±0.12	1.01±0.08
Test II		
	Absorption capacity (g water/g cotton)	Absorption capacity (g hexane/g cotton)
Cotton	2.12±0.08	0.08±0.02
TA-TDA	1.80±0.14	0.52±0.07
TA-HDA	1.27±0.05	0.85±0.04
TA-ODA	1.15±0.04	0.97±0.04

Table 8. The absorption capacity of fabrics modified with 5mM/19.6mM of $CuSO_4/H_2O_2$ in 10 min for water and hexane in Test II

Test II		
	Absorption capacity (g water/g cotton)	Absorption capacity (g hexane/g cotton)
TA-TDA	1.90±0.03	0.57±0.08
TA-HDA	1.32±0.08	0.82±0.06
TA-ODA	1.16±0.02	1.07±0.06

Table 9. The absorption capacity of fabrics modified with no $CuSO_4/H_2O_2$ in 10 min for water and hexane in Test II

Test II		
	Absorption capacity (g water/g cotton)	Absorption capacity (g hexane/g cotton)
TA-TDA	1.94±0.03	0.44±0.08
TA-HDA	1.46±0.10	0.72±0.07
TA-ODA	1.07±0.07	1.04±0.02

doi:10.6342/NTU202101615

4.3 The comparison of reaction conditions and performance for TA-ODA and POSS-CT

Based on the list in Table 1 and Table 3, we can realize that the cost of material for TA-ODA is 100 times much less than the compound for POSS-CT. Moreover, the industrial grade of tannic acid is much cheaper than the reagent grade used in experiment. It is cost-effective and shows great potential for practical application. Table 10 shows that the fabrication process of POSS-CT is complicated than TA-ODA used one step to carry out in 60 min. And it is energy-consuming to use UV equipment for synthesis. The halogenated solvent used for fabrication of POSS-CT is harmful to environment and human health. On the contrary, the solvent applied for TA-ODA is environmental-friendly for avoiding secondary pollution. For oil absorption capability, the performance of POSS-CT is similar with TA-ODA exhibiting outstanding oil absorption capability compared to the pristine cotton fabric. Consequently, the use of tannic acid-modified fabrics for oil absorption is more appropriate for large-scale production and environmental sustainability.

Table 10. The comparison of reaction conditions and performance for TA-ODA and POSS-CT

	TA-ODA	POSS-CT
Procedure	One step	Two step
Reaction condition	Room temperature pH 8.5	Room temperature UV irradiation (360 nm)
Reaction time	60 min	1^{st} step: 2hr 2^{nd} step: 60 min
Solvent	Water, Ethanol	Ethanol, Dichloromethane
Contact angle (°)	142.87±0.53	142.82±1.17
Oil absorption capacity	Test I : 1.01 Test II : 0.97	Test I : 0.96 Test II : 1.12

doi:10.6342/NTU202101615

Chapter 5
Conclusion

This study proposed a novel one step protocol to produce TA-TDA, TA-HDA and TA-ODA cotton fabrics by dip coating TA onto the surface together with the alkylamines onto the TA via Michael addition/Schiff base reactions. Moreover, the POSS-CT is introduced to do the comparative study which is fabricated by thiol-ene click reaction under the UV irradiation. The FTIR analysis, ^{1}H NMR, and XPS spectra confirmed the proposed chemical structures for the surface coating. The tannic acid-modified cotton fabrics have hydrophobic surfaces with contact angles for water droplets on the modified surface as 133.3^{o}, 136.0^{o} and 142.9^{o} for TA-TDA, TA-HDA, and TA-ODA cotton fabrics, respectively; and diiodomethane droplets on the modified surface being 56.0^{o}, 58.8^{o} and 59.3^{o}, respectively. The modified surfaces have low polar component (4.2-6.2 mJ/m^2) and intermediate dispersive component (29.0-31.2 mJ/m^2), generating a surface that has low affinity to water but high affinity to oil. The reaction parameters for Michael addition/Schiff base reactions including the reaction time, the concentrations of catalysts, and the solution pH values were studied on their effects for water contact angle to the modified surface. The two oil absorption tests revealed that the modified cotton fabrics can effectively absorb oil, with the adsorption capacity follows TA-ODA>TA-HDA>TA-TDA. Furthermore, the tannic acid-modified cotton fabric with no $CuSO_4/H_2O_2$ and short reaction time (10min) for fabrication also shows great oil absorption. The early contact of water will reduce the oil capacity since part of main pores have been occupied by water.

POSS-CT has superhydrophobic surface with contact angles for water droplets on the modified surface as 142.82° and diiodomethane droplets on the modified surface being 0°. The POSS-modified surfaces have polar component (13.3 mJ/m^2) and dispersive component (50.8 mJ/m^2) which is preferable to capture the oil compound instead of water. The reaction parameter for thiol-ene click reaction including the reaction time and concentration of POSS were adopt to realize the effect for hydrophobicity modification. The two oil absorption tests exhibited that the POSS-CT possessed great oil absorption capacity as well as tannic acid-modified cotton fabrics.

doi:10.6342/NTU202101615

Tannic acid-modified cotton fabrics show great potential for practical application owing to their low cost (Table 11), simple fabrication process and sustainable solvent medium compared to POSS-modified cotton fabric.

Table 11. The comparison of price for tannic acid, alkylamine, POSS and MPTES

Substance	Brand	Price
Tannic acid (ACS reagent grade)	Sigma-Aldrich	0.643 ($/g)
Tannic acid (Industrial grade, 67.5%)	Emperor Chemical	0.012 ($/g)
Octadecylamine (90%)	ACROS Organics	0.093 ($/g)
Hexadecylamine (90%)	ACROS Organics	0.100 ($/g)
Tetradecylamine (98%)	ACROS Organics	3.622 ($/g)
Octavinyloctasilasesquioxane (POSS)	TCI	51 ($/g)
(3-Mercaptopropyl)triethoxysilane (MPTES)	Sigma-Aldrich	4.86 ($/ml)

Data from Sigma-Aldrich, Emperor Chemical, ACROS Organics and TCI

doi:10.6342/NTU202101615

References

[1] Zhang X., Li Z., Liu K. and Jiang L., Bioinspired Multifunctional Foam with Self-Cleaning and Oil/Water Separation, Adv. Funct. Mater. 2013. 23, 2881-2886

[2] Boo C., Lee J. and Menachem E., Omniphobic Polyvinylidene Fluoride (PVDF) Membrane for Desalination of Shale Gas Produced Water by Membrane Distillation, Environ. Sci. Technol. 2016. 50, 12275-12282

[3] Wang H., Zhang C., Zhou B., Zhang Z., Shen J. and Du A., Hydrophobic Silica Nanorod Arrays Vertically Grown on Melamine Foams for Oil/Water Separation, Appl. Nano Mater. 2020. 3, 1479-1488

[4] Jayaprakash S., Kavithaa L. and Sarper S., An overview of oil-water separation using gas flotation systems, Chemosphere 2016. 144, 671-680

[5] Lü T., Qi D., Zhang D., Fu K., Li Y. and Zhao H., Fabrication of recyclable multi-responsive magnetic nanoparticles for emulsified oil-water separation, J. of C. Prod., 2020. 255, 120293

[6] Shang Q., Liu C. and Zhou Y., One-pot fabrication of robust hydrophobia and superoleophilic cotton fabrics for effective oil-water separation, J. Coat. Technol. Res., 2018. 15, 65-75

[7] Love D., Madhabendra R. and Partha S., Reduced graphene oxide-coated cotton as an efficient absorbent in oil-water separation, Ad. Com. and Hy. Mat. 2018. 1, 135-148

[8] Singh A. K. and Singh J. K., An efficient use of waste PE for hydrophobic surface coating and its application on cotton fibers for oil-water separator, Pro. in Org. Co., 2019. 131, 301–310

doi:10.6342/NTU202101615

[9] Love D., Dibya D. B. and Partha S., Methyltrichlorosilane functionalized silica nanoparticles-treated superhydrophobic cotton for oil-water separation, J. Coat. Technol. Res. 2019. 16, 1021-1032

[10] Arun K. S. and Jayant K. S., An efficient use of waste PE for hydrophobic surface coating and its application on cotton fibers for oil-water separator, Pro. in Org. Coat. 2019. 131, 301-310

[11] Yang Y., Li X., Zheng X., Chen Z., Zhou Q. and Chen Y., 3D-Printed Biomimetic Super-Hydrophobic Structure for Microdroplet Manipulation and Oil/Water Separation, Adv. Mater. 2018. 30, 1704912

[12] Nurul A. I., Nurin W. M. Z., Zaira Z. C. and Mohd R. J., Grafting of straight alkyl chain improved the hydrophobicity and tribological performance of graphene oxide in oil as lubricant, Jo. of Mol. Liq. 2020. 319, 114276

[13] Gu J., Jiang W., Wang F., Chen M., Mao J. and Xie T., Facile removal of oils from water surfaces through highly hydrophobic and magnetic polymer nanocomposites, Appl. Sur. Sci. 2014. 301, 492-499

[14] Cho Y. K., Park E. J. and Kim Y. D., Removal of oil by gelation using hydrophobic silica nanoparticles, Jo. of Ind. And Eng. Che. 2014. 20, 1231-1235

[15] Lin T. C. and Lee D. J., Cotton fabrics modified for use in oil/water separation:a perspective review, Cellulose 2021.

[16] Chen W., Vikram K., Thomas N. H. C., Siti S. R. and Jerry Y. Y. H., Surface hydrophobicity: effect of alkyl chain length and network homogeneity, Fron. of Che. Sci. and Eng. 2021. 15, 90-98

[17] Hongxia W., Hua Z., Adrian G., Jian F., Haitao N., Jie D. and Tong L., Robust, electro-conductive, self-healing superamphiphobic fabric prepared by one-step vapour-phase polymerisation of poly(3,4-ethylenedioxythiophene)

doi:10.6342/NTU202101615

in the presence of fluorinated decyl polyhedral oligomeric silsesquioxane and fluorinated alkyl silane, Soft Matter. 2013. 9, 277-282

[18] Pan G., Xiao X. and Ye Z., Fabrication of stable superhydrophobic coating on fabric with mechanical durability, UV resistance and high oil-water separation efficiency, Sur. and Coat. Tech.,c2019. 360, 318-328

[19] Yang D., Di H., Yi Y. D., Q. Zhang ,Feng C. and Qiang F., Facile one-step preparation of robust hydrophobic cotton fabrics by covalent bonding polyhedral oligomeric silsesquioxane for ultrafast oil/water separation, Che. Eng. Jo., 2020. 379, 122391

[20] Kazuo T. and Yoshiki C., Advanced functional materials based on polyhedral oligomeric silsesquioxane (POSS), J. Mater. Chem. 2012. 22, 1733-1746

[21] Lin F., Wang Z., Shen Y., Tang L., Zhang P., Wang Y., Chen Y., Huang B. and Lu B., Natural skin-inspired versatile cellulose biomimetic hydrogels, J. Mater. Chem. A. 2019. 7, 26442-26455

[22] Kim S., Gim T. and Kang S. M., Versatile, Tannic Acid-Mediated Surface PEGylation for Marine Antifouling Applications, ACS Appl. Mater. Interfaces 2015. 7, 6412–6416

[23] Li Y., Feng Z., He Y., Fan Y., Ma J. and Yin X., Facile way in fabricating a cotton fabric membrane for switchable oil/water separation and water purification, Appl. Sur. Sci. 2018. 411, 500-507

[24] Yan X., Zhu X., Ruan Y., Xing T., Chen G. and Zhou C., Biomimetic, dopamine-modified superhydrophobic cotton fabric for oil–water separation, Cellulose 2020. 27, 7873-7885

[25] Wang Z., Ji S., Zhang J., Liu Q., He F., Peng S. and Li Y., Tannic acid encountering ovalbumin: a green and mild strategy for superhydrophilic and underwater superoleophobic modification of various hydrophobic

doi:10.6342/NTU202101615

membranes for oil/water separation, J. Mate. Chem. A 2018. 6, 13959−13967

[26] Feng S, Li M, Zhang S, Zhang Y, Wang B, Wu L (2019) Superoleophobic micro-nanostructure surface formation of PVDF membranes by tannin and a condensed silane coupling agent. RSC Adv 9: 32021–32026

[27] Gu S., Yang L., Huang W., Bu Y., Chen D., Huang J., Zhou Y. and Xu W., Fabrication of hydrophobic cotton fabrics inspired by polyphenol chemistry, Cellulose 2017. 24, 2635–2646

[28] Sun Y., Huang J., Zhao J. and Guo Z., Fabrication of durable self-repairing superhydrophobic fabrics via a fluorinate-free waterborne biomimetic silicification strategy, New J. Chem. 2019. 43, 5032-5038

[29] He Y., Chen Q., Zhang Y. Zhoa Y. and Chen L., H_2O_2-Triggered Rapid Deposition of Poly(caffeic acid) Coatings: A Mechanism-Based Entry to Versatile and High-Efficient Molecular Separation, ACS Appl. Mater. Interfaces 2020. 12, 52104−52115

[30] Sun M., Guo H., Zheng J., Wang Y., Liu X., Li Q., Wang R. and Jia X., Hydrophobic octadecylamine-polyphenol film coated slow released urea via one-step spraying co-deposition, Pol. Te. 2020. 91, 106831

[31] Lui Y., Tang J., Wang R., Lu H., Li L., Kong Y., Qi K. and Xin J. H., Artificial lotus leaf structures from assembling carbon nanotubes and their applications in hydrophobic textiles, Jo. of Mat. Che., J. Mater. Chem. 2007.17, 1071-1078

[32] Shao Y., Zhao J., Fan Y., Wan Z., Lu L., Zhang Z., Ming W. and Ren L., Shape Memory Superhydrophobic Surface with Switchable Transition between“Lotus Effect” to “Rose Petal Effect”, Ch. Eng. Jo. 2020. 382, 122989

doi:10.6342/NTU202101615

[33] Gregory D. B. and Bharat B., Rice- and Butterfly-Wing Effect Inspired Self-Cleaning and Low Drag Micro/Nanopatterned Surfaces in Water, Oil, and Air Flow. Nanoscale 2014. 6, 76−96

[34] Sanjay S. L., Rajaram S. S., Vishnu S. K., Bhosale A.K., A. M. Kumar, Kishor K. S., Ruimin X. and Liu S., Self-cleaning superhydrophobic coatings: Potential industrial applications, Pro. in org. Co. 2019. 128, 52-58

[35] Lim J. I., Kang M. J. and Lee W. K., Lotus-leaf-like structured chitosan–polyvinyl pyrrolidone films as an anti-adhesion barrier, Appl. Sur. Sci. 2014. 320, 614-619

[36] Fang Y., Sun G., Bi Y. and Zhi H., Multiple-dimensional micro/nano structural models for hydrophobicity of butterfly wing surfaces and coupling mechanism, Sci. Bul. 2015. 60, 256-263

[37] Kerstin K., Bharat B. , Jung Y. C. and Wilhelm B., Fabrication of artificial Lotus leaves and significance of hierarchical structure for superhydrophobicity and low adhesion, Soft Matter, 2009. 5, 1386-1393

[38] Daniel E. and Bharat B., Durable Lotus-effect surfaces with hierarchical structure using micro- and nanosized hydrophobic silica particles, Jo. of Col. and Int. Sci. 2012. 368, 584-591

[39] Zhang W., Yu Z., Chen Z. and Li M., Preparation of super-hydrophobic Cu/Ni coating with micro-nano hierarchical structure, Mat. Let. 2012. 67, 327-330

[40] Dai S., Zhang D., Shi Q., Han X., Wang S. and Du Z., Biomimetic fabrication and tunable wetting properties of three-dimensional hierarchical ZnO structures by combining soft lithography templated with lotus leaf and hydrothermal treatments, CrystEngComm. 2013. 15, 5417–5424

doi:10.6342/NTU202101615

[41] Andrew K., Li Z., Caitlyn C., Rebecca M., Shonali D., Vahid V., Zhou F., Brian D., Liu H., and Li L., Study on the Surface Energy of Graphene by Contact Angle Measurements, Langmuir 2014. 30, 8598–8606

[42] Krasowska M., Zawala J. and Malysa K. Air at hydrophobic surfaces and kinetics of three phase contact formation, Adv. in Coll. and Int. Sci. 2009. 147–148, 155–169

[43] Kwok D.Y. and Neumann A.W., Contact angle measurement and contact angle interpretation. Adv. in Col. and Int. Sci. 1999. 81, 167-249

[44] Arun K. S. and Jayant K. S., Fabrication of durable super-repellent surfaces on cotton fabric with liquids of varying surface tension: Low surface energy and high roughness, Appl. Sur. Sci. 2017. 416, 639-648

[45] Zhuang Y. X. and Ole H., Correlation of Effective Dispersive and Polar Surface Energies in Heterogeneous Self-Assembled Monolayer Coatings, Langmuir 2009. 25(10), 5437–5441

[46] Wu S., Calculation of interfacial tension in polymer systems, J. Pol. Sci.: Part C 1971. 34, 19-30

[47] Shannon M. N. and Magnus N., Surface Energy and Wettability of Spin-Coated Thin Films of Lignin Isolated from Wood, Langmuir 2010. 26(8), 5484-5490

[48] Owens D. K. and Wendt R. C., Estimation of the surface free energy of polymers, Jo of Appl. Pol. Sci. 1969. 13, 1741-1747

[49] Pinho E. and Soares G., Functionalization of cotton cellulose for improved wound healing, J. Mater. Chem. B 2018. 6, 1887--1898

[50] He T., Zhao H., Liu Y., Zhao C., Wang L., Wang H., Zhao Y. and Wang H., Facile fabrication of superhydrophobic Titanium dioxide-composited cotton fabrics to realize oil-water separation with efficiently photocatalytic

doi:10.6342/NTU202101615

degradation for water-soluble pollutants, Col. and Sur. A, 2020. 585(20), 124080

[51] Mai Z., Xiong Z., Shu X. , Liu X., Zhang H., Yin X. , Zhou Y., Liu M., Zhang M., Xu W. and Chen D., Multifunctionalization of cotton fabrics with polyvinylsilsesquioxane/ZnO composite coatings, Car. Pol., 2018. 199(1), 516-525

[52] Yang M., Liu W., Liang L., Jiang C., Liu C., Xie Y., Shi H., Zhang F. and Pi K., A mild strategy to construct superhydrophobic cotton with dual self-cleaning and oil–water separation abilities based on TiO_2 and POSS via thiol-ene click reaction, Cellulose 2020. 27, 2847-2857

[53] He Y., Wan M., Wang Z., Zhang X., Zhao Y. and Sun L., Fabrication and characterization of degradable and durable fluoride-free super-hydrophobic cotton fabrics for oil/water separation, Sur. and Co. Tech., 2019. 378, 125079

[54] Wang J., Geng G., Wang A., Liu X., Du J., Zou Z., Zhang S. and Han F., Double biomimetic fabrication of robustly superhydrophobic cotton fiber and its application in oil spill cleanup, Ind. Cro. And Pro. 2015. 77, 36-43

[55] Marcin P., Hieronim M.and Agnieszka D., Preparation of highly hydrophobic cotton fabrics by modification with bifunctional silsesquioxanes in the sol-gel process, Appl. Sur. Sci. 2016. 387, 163-174

[56] Ricardo M., Josep M. T., Kan C. W., and Petar J., Hydrophobic Coatings on Cotton Obtained by in Situ Plasma Polymerization of a Fluorinated Monomer in Ethanol Solutions, ACS Appl. Mater. Interfaces 2017. 9, 5513–5521

[57] Dawid P., Agnieszka M. and Ewa A., POSS-modified UV-curable coatings with improved scratch hardness and hydrophobicity, Pro. in Org. Coat. 2016. 100, 165-172

doi:10.6342/NTU202101615

[58] Huang S., Zhang Y., Shi J. and Huang W., Superhydrophobic particles derived from nature-inspired polyphenol chemistry for liquid marble formation and oil spills treatment, ACS Sustain. Chem. Eng. 2016. 4, 676−681.

[59] Liu F., Ma M., Zang D., Gao Z. and Wang C., Fabrication of superhydrophobic/superoleophilic cotton for application in the field of water/oil separation, Carbohyd. Polym. 2014. 97, 59–64.

[60] Zhang M., Wang C., Wang S. and Li J.. Fabrication of superhydrophobic cotton textiles for water–oil separation based on drop-coating route, Carbohyd. Polym. 2013. 97, 59−64

[61] Xu B., Cai Z., Wang W. and Ge F., Preparation of superhydrophobic cotton fabrics based on SiO_2 nanoparticles and ZnO nanorod arrays with subsequent hydrophobic modification, Sur. and Coat. Tech. 2010. 20, 1556-1561

[62] Boticas I., Dias D., Ferreira1 D., Magalhães P., Silva R., Fangueiro R. 2019. Superhydrophobic cotton fabrics based on ZnO nanoparticles functionalization, SN App. Sci. 2019. 1, 1376

[63] Li S., Huang J., Ge M., Cao C., Deng S., Zhang S., Chen G., Zhang K., Salem S. A. and Lai Y., Robust Flower-Like TiO_2@Cotton Fabrics with Special Wettability for Effective Self-Cleaning and Versatile Oil/Water Separation, Adv. Mater. Interfaces 2015. 2, 1500220

[64] Zhang J., France P., Arseni R., Saswati D., Zhao J. and William V. O., Hydrophobic cotton fabric coated by a thin nanoparticulate plasma film, Jo. of App. Poly. Sci. 2003. 88, 1473-1481

[65] Shen L., Pan Y. and Fu H., Fabrication of UV curable coating for super hydrophobic cotton fabrics, Appl. Poly. 2019. 59, 452-459

[66] Cao C., Ge M., Huang J., Li S., Deng S., Zhang S., Chen Z., Zhang K., Salem S. A. D. and Lai Y., Robust fluorine-free superhydrophobic PDMS–

doi:10.6342/NTU202101615

ormosil@fabrics for highly effective self-cleaning and efficient oil–water separation, Jo. of Mat. Che. A 2016. 4, 12179–12187

[67] Guo H, Yang J., Xu T., Zhao W., Zhang J., Zhu Y., Wen C., Li Q., Sui X. and Zhang L., A Robust Cotton Textile-Based Material for High-Flux Oil−Water Separation, ACS Appl. Mater. Interfaces 2019. 11, 13704−13713

[68] Sourav M., Sukanta P., Ananya C. and Jayanta M., Fabrication of fluoropolymer-modified hydrophobic functionalization of cotton fabric by admicellar polymerization, Sur. Eng. 2019. 110, 1-8

[69] Yu Y., Wang Q., Yuan J., Fan X., Wang P. and Cui L., Hydrophobic modification of cotton fabric with octadecylamine via laccase/TEMPO mediated grafting, Car. Poly. 2016. 137, 549-555

[70] Gao Q., Zhu Q., Guo Y., and Yang C. Q., Formation of Highly Hydrophobic Surfaces on Cotton and Polyester Fabrics Using Silica Sol Nanoparticles and Nonfluorinated Alkylsilane, Ind. Eng. Chem. Res. 2009. 48, 9797–9803

[71] Gu Z. Z., Akira F. and Osamu S., Patterning of a Colloidal Crystal Film on a Modified Hydrophilic and Hydrophobic Surface, Ind. Eng. Chem. Res. 2009. 48, 9797–9803

[72] Wang C., Yao T., Wu J., Ma C., Fan Z., Wang Z., Cheng Y., Lin Q. and Yang B., Facile approach in fabricating superhydrophobic and superoleophilic surface for water and oil mixture separation. ACS Appl. Mater. Interf. 2009. 11, 2613−2617.

[73] Muhammad Z. K., Vijay B., Jiri M., Azam A. and Martina V., Superhydrophobicity, UV protection and oil/water separation properties of fly ash/Trimethoxy(octadecyl)silane coated cotton fabrics, Carb. Poly. 2018. 202, 571-580

doi:10.6342/NTU202101615

[74] Qi Y., Chen S. and Zhang J., Fluorine modification on titanium dioxide particles: Improving the anti-icing performance through a very hydrophobic surface. Appl. Surf. Sci. 2019. 476, 161−173

[75] Xue Q., Cao H., Meng F., Quan M. and Gong Y. K., Cell membrane mimetic coating immobilized by mussel-inspired adhesion on commercial ultrafiltration membrane to enhance antifouling performance, Jo. of Mem. Sci. 2017., 528(15), 1-10

[76] Lee H., Shara M. D., William M. M. and Philip B. M., Mussel-inspired surface chemistry for multifunctional coatings, Science, 2007. 318(5849), 426–430

[77] Hu M. X., Yang Q. and Xu Z. K., Enhancing the hydrophilicity of polypropylene microporous membranesby the grafting of 2-hydroxyethyl methacrylate via a synergistic effect of photoinitiators, Jo. of Mem. Sci., 2006 285(1-2), 196–205

[78] Chen X., Huang G., An C., Feng R., Yao Y., Zhao S., Huang C. and Wu Y., Plasma-induced poly(acrylic acid)-TiO_2 coated polyvinylidenefluoridemembrane for produced water treatment: Synchrotron X-Ray,optimization, and insight studies, Jo. of Cle. Prod., 2019. 227(1), 772-783

[79] Zhang R. X., Braeken L., Luis P., Wang X. L. and Bart Van der Bruggen, Novel binding procedure of TiO_2 nanoparticles to thin film composite membranes via self-polymerized polydopamine, Jo. of Mem. Sci., 2013. 437, 179-188

[80] Yang J., Xu H., Zhang L., Zhong Y., Sui X. and Mao Z., Lasting superhydrophobicity and antibacterial activity of Cu nanoparticles

doi:10.6342/NTU202101615

immobilized on the surface of dopamine modified cotton fabrics, Sur. And Co. Tech., 2017. 309(15), 149-154

[81] Zhoa X., Jia N., Cheng L., Liu L. and Gao C., Dopamine-induced biomimetic mineralization for in situ developing antifouling hybrid membrane, Jo. of Mem. Sci., 2018. 560(15), 47-57

[82] Zeng G., Ye Z., He Y., Yang X., Ma J., Shi H. and Feng Z., Application of dopamine-modified halloysite nanotubes/PVDF blend membranes for direct dyes removal from wastewater, Che. Eng. Jo., 2017. 323(1) 572-583

[83] Liu Y., Gan D., Chen M., Ma L., Yang B., Li L., Zhu M. and Tu W., Bioinspired dopamine modulating graphene oxide nanocomposite membrane interposed by super-hydrophilic UiO-66 with enhanced water permeability, Sep. and Pur. Tech., 2020. 253(15), 117552

[84] Muchtar S., Wahab M. Y.,, Mulyati S., Arahman N. and Riza M., Superior fouling resistant PVDF membrane with enhanced filtration performance fabricated by combined blending and the self-polymerization approach of dopamine, Jo. of W. Pro. Eng., 2019. 28, 293-299

[85] Chen S., Chen Y., Lei Y. and Yin Y., Novel strategy in enhancing stability and corrosion resistance for hydrophobic functional films on copper surfaces, Elec. Com., 2009. 11, 1675-1679

[86] Dan Z., Guolin Z., Chung Z., Yuhe W. and Zhu L., Preparation and characterization of wear-resistant superhydrophobic cotton fabrics, Pro. In Org. Co., 2019. 134, 226-233

[87] Qiu W. Z., Yang H C. and Xu Z. K., Dopamine-assisted co-deposition: An emerging and promising strategy for surface modification, Adv. in Co. and Int. Sci., 2018. 256, 111-125

doi:10.6342/NTU202101615

[88] Chen S., Xie Y., Xiao T., Zhao W., Li J. and Zhao C., Tannic acid-inspiration and post-crosslinking of zwitterionic polymer as a universal approach towards antifouling surface, Chem. Eng. Jo., 2018. 337(1), 122-132

[89] Liao C., Xu Q., Wu C., Fang D., Chen S., Chen S., Luo J. and Li L., Core–shell nano-structured carbon composites based on tannic acid for lithium-ion batteries, J. Mater. Chem. A 2016. 4, 17215-17224

[90] Zhang M., Cheng C., Guo C., Jin L., Liu L., Li M., Shang L., Lui Y. and Ao Y., Co-depositing bio-inspired tannic acid-aminopropyltriethoxysilane coating onto carbon fiber for excellent interfacial adhesion of epoxy composites,Co,. Sci. and Tech., 2021 204(1), 109639

[91] Peng H., Wang D. and Fu S., Tannic acid-assisted green exfoliation and functionalization of MoS2 nanosheets: Significantly improve the mechanical and flame-retardant properties of polyacrylonitrile composite fibers, Che. Eng. Jo., 2020. 384, 123288

[92] Wang T., Ma B., Jin A., Li X., Zhang X., Wang W. and Cai Y., Facile loading of Ag nanoparticles onto magnetic microsphere by the aid of a tannic acid-Metal polymer layer to synthesize magnetic disinfectant with high antibacterial activity, Jo. of Haz. Mat., 2018. 342(15), 392-400

[93] Kim T.Y., Cha S.H., Cho S. and Park Y., Tannic acid-mediated green synthesis of antibacterial silver nanoparticles, Arch. Pharm. Res., 2016. 39, 465–473

[94] İlhami G., Zübeyr H., Mahfuz E. and Hassan Y. A., Radical scavenging and antioxidant activity of tannic acid, Ar. Jo. of Che., 2010. 2(1), 43-53

[95] Jiao S., Jin J. and Wang L., Tannic acid functionalized N-doped graphene modified glassy carbon electrode for the determination of bisphenol A in food package, Tal. 2014. 122, 140-144

doi:10.6342/NTU202101615

[96] Zhang Z. Y., Zheng Y. D., He.W., Yang Y. Y., Xie Y. J., Feng Z. X. and Qiao K., A biocompatible bacterial cellulose/tannic acid composite with antibacterial and anti-biofilm activities for biomedical applications Mat. Sci. and Eng., 2020. 106, 110249

[97] Lim M. Y., Choi. Y. S., Kim J., Kim. K., Shin H., Kim J. J., Shin D. M. and Lee J. C., Cross-linked graphene oxide membrane having high ion selectivity and antibacterial activity prepared using tannic acid-functionalized graphene oxide and polyethyleneimine, Jo. of Mem. Sci., 2017. 521(1), 1-9

[98] Zhang X., My D. D., Philip C., Adrian S., Greg G. Q., Leif L., Peter L. and Shantha K., Chemical Modification of Gelatin by a Natural Phenolic Cross-linker, Tannic Acid, J. Agric. Food Chem. 2010. 58(11), 6809–6815

[99] Viyapuri R., Thomas A. W., Chee C. Y. and Praveena N., Physical and chemical reinforcement of chitosan film using nanocrystalline cellulose and tannic acid, Cellulose 2015. 22, 2529-2541

[100] Xu Y., Guo D., Li Y., Xioa Y., Shen L., Li R. Jiao Y. and Lin H., Manipulating the mussel-inspired co-deposition of tannic acid and amine for fabrication of nanofiltration membranes with an enhanced separation performance, Jo. of Col. and Int. Sci., 2020. 565(1), 23-34

[101] Li Y., Shi S., Cao H. and Cao R., Robust antifouling anion exchange membranes modified by graphene oxide (GO)-enhanced Co-deposition of tannic acid and polyethyleneimine, 2021. 625, 119111

[102] Li Q., Liao Z., Fang X., Xie J., Ni L., Wang D., Qi J., Sun X., Wang L. and Li J., Tannic acid assisted interfacial polymerization based loose thin-film composite NF membrane for dye/salt separation, Desalination, 2020. 479(1), 114343

doi:10.6342/NTU202101615

[103] Zhang X., Ren P. F., Yang H. C., Wan L.S. and Xu Z. K., Co-deposition of tannic acid and diethlyenetriamine for surface hydrophilization of hydrophobic polymer membranes, App. Sur. Sci., 2016. 360(1) 291-297

[104] Tham H. M. and Chung T. S., One-step cross-linking and tannic acid modification of polyacrylonitrile hollow fibers for organic solvent nanofiltration, Jo. of Mem. Sci., 2020. 610, 118294.

[105] Huang Y., Lin Q., Yu Y. and Yu W., Functionalization of wood fibers based on immobilization of tannic acid and in situ complexation of Fe (II) ions, Appl. Sur. Sci., 2020. 510(30), 145436

[106] Xu G., Dicky P., Zhang B., Xu L., Neoh K. G. and Kang E. T., Tannic acid anchored layer-by-layer covalent deposition of parasin I peptide for antifouling and antimicrobial coatings, RSC Adv., 2016. 6, 14809

[107] Wang Z., Ji S., He F., Cao M., Peng S. and Li Y., One-step transformation of highly hydrophobic membranes into superhydrophilic and underwater superoleophobic ones for high-efficiency separation of oil-in-water emulsions, J. Mater. Chem. A, 2018. 6, 3391-3396

[108] Bu Y., Zhang S., Cai Y., Yang Y., Ma S., Huang J., Yang H., Ye D., Zhou Y., Xu W. and Gu S., Fabrication of durable antibacterial and superhydrophobic textiles via in situ synthesis of silver nanoparticle on tannic acid-coated viscose textiles, Cellulose, 2018. 26, 2109-2122

[109] Shang Q., Hu L., Yang X., Hu Y., Bo C., Pan Z., Ren X., Liu C. and Zhou Y., Superhydrophobic cotton fabric coated with tannic acid/polyhedral oligomeric silsesquioxane for highly effective oil/water separation, Pro. In Or. Co., 2021. 154, 106191

doi:10.6342/NTU202101615

[110] Zahouily M., Abrouki Y., Bahlaouan B., Rayadh A. and Sebti S., Hydroxyapatite: new efficient catalyst for the Michael addition, Cat. Com. 2003. 4(10) 521-524

[111] Zhu Y., Jeremiah P. M., Viresh H. and Rawai P., Squaramide-Catalyzed Enantioselective Michael Addition of Diphenyl Phosphite to Nitroalkenes, Angew. Chem. 2010. 122, 157-160

[112] Chatani S., Devatha P. N. and Christopher N. B., Relative reactivity and selectivity of vinyl sulfones and acrylates towards the thiol–Michael addition reaction and polymerization, Pol. Chem. 2013. 4, 1048-1055

[113] Brian D. M., Kalpana V., Kevin M. M. and Timothy E. L., Michael addition reactions in macromolecular design for emerging technologies, Prog. Polym. Sci. 2006. 31, 487–531

[114] Andrew M. and Jeffrey H., Network Formation and Degradation Behavior of Hydrogels Formed by Michael-Type Addition Reactions, Bio. 2005. 6(1), 290–301

[115] Devatha P. N., Maciej P., Shunsuke C., Gong T., Xi W., Christopher R. F. and Christopher N. B., The Thiol-Michael Addition Click Reaction: A Powerful and Widely Used Tool in Materials Chemistry, Chem. Mater. 2014. 26, 724−744

[116] Li G. Z., Rajan K. R., Alexander H. S., Gregory R., Cyrille B., Tong Z., Thomas P. D., C. Remzi B. and David M. H., Investigation into thiol-(meth)acrylate Michael addition reactions using amine and phosphine catalysts, Poly. Che. 2010. 1, 1196-1204

[117] Moorthy N. V. G., Rajendar D., and Sunil V. P., Formal Synthesis of (+)-Lasubine II and (−)-Subcosine II via Organocatalytic Michael Addition of a Ketone to an α-Nitrostyrene, Org. Lett. 2015. 17(21), 5312–5315

doi:10.6342/NTU202101615

[118] Wang Y., Li P., Liang X. and Ye J., Base–Base Bifunctional Catalysis: A Practical Strategy for Asymmetric Michael Addition of Malonates to α,β-Unsaturated, Aldehydes, Adv. Synth. Catal. 2008. 350, 1383–1389

[119] David M., Silvia D., Pablo B., Rosario F. and José M. L., Synthesis of enantioenriched azo compounds: organocatalytic Michael addition of formaldehyde N-tert-butyl hydrazone to nitroalkenes, Org. Biomol. Chem., 2013. 11, 326-335

[120] Xi W., Peng H., Alan A. S., Christopher J. K., Jeffery W. S., and Christopher N. B., Spatial and Temporal Control of Thiol-Michael Addition via Photocaged Superbase in Photopatterning and Two-Stage Polymer Networks Formation, Macromolecules 2014. 47, 6159–6165

[121] Christian H., Mihaiela C. S., Anders D. and Anzar K., Aza-Michael addition reaction: Post-polymerization modification and preparation of PEI/PEG-based polyester hydrogels from enzymatically synthesized reactive polymers, Pol. Che. 2015. 53, 745-749

[122] Han S. C., He W. D., Li J., Li L. Y., Sun X. L., Zhang B. Y. and Pan T. T., Reducible polyethylenimine hydrogels with disulfide crosslinkers prepared by michael addition chemistry as drug delivery carriers: Synthesis, properties, and in vitro release, Pol. Che. 2009. 47, 4047-4082

[123] Liu J., Li J., Yu F., Zhao Y. X., Mo X. M. and Pan J. F., In situ forming hydrogel of natural polysaccharides through Schiff base reaction for soft tissue adhesive and hemostasis, Int. Jo. of Bio.Macro. 2020. 147, 653-666

[124] Hossein N., Fariba S. and Khadigeh R., Mild and convenient one pot synthesis of Schiff bases in the presence of P_2O_5/Al_2O_3 as new catalyst under solvent-free conditions, Jo. of Mol. Cat. 2006. 260, 100-104

doi:10.6342/NTU202101615

[125] Jia Y. and Li J., Molecular Assembly of Schiff Base Interactions: Construction and Application, Chem. Rev. 2015. 115, 1597−1621

[126] Jia Y., Fei J., Cui Y., Yang Y., Gao L. and Li J., pH-responsive polysaccharide microcapsules through covalent bonding assembly,) Chem. Commun. 2011. 47, 1175-1177

[127] Xin Y. and Yuan J., Schiff's base as a stimuli-responsive linker in polymer chemistry, Polym. Chem. 2012. 3, 3045

[128] Xiang S., Yang J., Cui Z., Qin S. and Qin Q., Preparation of hollow fiber membrane via grafting tannic acid and its influence on microstructure, permeability and anti-fouling, Mat. Let. 2021. 285, 129095

[129] Xu J., Liu Y. and Hsu S. H., Hydrogels Based on Schiff Base Linkages for Biomedical Applications, Mol. 2019. 24(16), 3005

[130] Ding Y. H., Floren M. and Tan W., Mussel-inspired polydopamine for bio-surface functionalization, Bio. and Bio., 2016. 2(4), 121-136

[131] Liu X., Cao J., Li H. Li J., Jin Q.,Ren K. and Ji J., Mussel-Inspired Polydopamine: A Biocompatible and Ultrastable Coating for Nanoparticles in Vivo, ACS Nano, 2013. 7(10), 9384-9395

[132] Ryou M. H., Lee Y. M., Park J.K. and Choi J. W., Mussel-Inspired Polydopamine-Treated Polyethylene Separators for High-Power Li-Ion Batteries, Adv. Mater., 2011. 23, 3066–3070

[133] Chen Y. and Liu Q., Oxidant-induced plant phenol surface chemistry for multifunctionalcoatings: Mechanism and potential applications, Jo. of Mem. Sci. 2019. 570-571, 176-183

[134] Jiang C., Liu W., Yang M., Liu C., He S., Xie Y. and Wang Z., Robust multifunctional superhydrophobic fabric with UV induced reversible

doi:10.6342/NTU202101615

wettability, photocatalytic self-cleaning property, and oil-water separation via thiol-ene click chemistry, Appl. Surf. Sci. 2019. 463, 34−44.

[135] Jannatun N., Taraqqi-A-Kamal, A., Rehman R., Kuker J. and Kumar Lahiri S., A facile cross-linking approach to fabricate durable and self-healing superhydrophobic coatings of SiO_2-PVA@PDMS on cotton textile, Euro. Poly. Jour. 2020. 134(5), 109836

[136] Li Y., Zhang Y., Zou C. and Shao J., Study of plasma-induced graft polymerization of stearyl methacrylate on cotton fabric substrates, App. Sur. Sci. 2015. 357, 2327-2332

[137] Du X., Li L., Li J., Yang C., Frenkel N., Welle A., Heissler S., Nefedov A., Grunze M. and Levkin P. A., UV-Triggered Dopamine Polymerization: Control of Polymerization, Surface Coating, and Photopatterning, Adv. Mater., 2014. 26, 8029–8033

[138] Cai J., Huang J., Ge M., Iocozzia J.,Lin Z., Zhang K. Q. and Lai Y., Immobilization of Pt Nanoparticles via Rapid and Reusable Electropolymerization of Dopamine on TiO_2 Nanotube Arrays for Reversible SERS Substrates and Nonenzymatic Glucose Sensors, Small 2017. 13, 1604240

[139] Lee M., Lee S. H., Oh I. K. and Lee H., Microwave-Accelerated Rapid, Chemical Oxidant-Free, Material-Independent Surface Chemistry of Poly(dopamine), Small 2017. 13, 1600443

[140] Zhang C., Li H. N., Du Y., Ma M. Q., and Xu Z. K., $CuSO_4/H_2O_2$-Triggered Polydopamine/Poly(sulfobetaine methacrylate) Coatings for Antifouling Membrane Surfaces, Langmuir, 2017. 33, 1210−1216

[141] Zhang C., Ou Y., Lei W.Xi, Wan L. S., Ji J. and Xu Z. K., CuSO4/H2O2-Induced Rapid Deposition of Polydopamine Coatings with

doi:10.6342/NTU202101615

High Uniformity and Enhanced Stability, Angew.Chem. Int. Ed., 2016. 55,3054 –3057

[142] Farid B. S., Zhang H., Vanessa T., Alexander W., Nicolas P. and Pavel A. L., UV-Triggered Polymerization, Deposition, and Patterning of Plant Phenolic Compounds, Adv. Funct. Mater. 2017. 27, 1700127

[143] Charles E. H. and Christopher N. B., Thiol–Ene Click Chemistry, Angew. Chem. Int. Ed. 2010. 49, 1540-1573

[144] Alexander K. T. S., Richard A. F., and Robin L. G., Thiol-ene Click Reaction as a General Route to Functional Trialkoxysilanes for Surface Coating Applications, J. Am. Chem. Soc. 2011. 133, 11026–11029

[145] Ke Y., Xingyi H., Ming Z., Liyuan X., Toshikatsu T., and Pingkai J., Combining RAFT Polymerization and Thiol−Ene Click Reaction for Core−Shell Structured Polymer@BaTiO3 Nanodielectrics with High Dielectric Constant, Low Dielectric Loss, and High Energy Storage Capability, ACS Appl. Mater. Interfaces 2014. 6, 1812-1822

[146] Di S., Wei W. and Dan Y., Preparation of fluorine-free water repellent finishing via thiol-ene click reaction on cotton fabrics, Mat. Let. 2016. 185, 514-518

[147] Mustafa U., Mehmet A. T., Yusuf Y., Influence of Type of Initiation on Thiol–Ene ‘‘Click’’ Chemistry, Macromol. Chem. Phys. 2010. 211, 103–110

[148] Oğuz T. and Michael A. R. M., The thiol-ene (click) reaction for the synthesis of plant oil derived polymers, Eur. J. Lipid Sci. Technol. 2013. 115, 41–54

[149] Lei X., Yanyan Z., Yujing Z., Shen D., Jie Z. and Shengyu F., Preparation and characterization of novel UV-curing silicone rubber viathiol-ene reaction, Mat. Let. 2013. 103, 425-427

doi:10.6342/NTU202101615

[150] Amanda B., Mack B., Tanner H., Mohammad I. H., T. Grant G., Kevin N. W., and Christy W. W., Superhydrophobic Functionalization of Cotton Fabric via Reactive Dye Chemistry and a Thiol−ene Click Reaction, : Ind. Eng. Chem. Res. 2019. 58, 22534−22540

[151] Bin L., Xiaoran D., Zhongxi X., Ziyong C., Piaoping Y. and Jun L., Thiol–Ene Click Reaction as a Facile and General Approach for Surface Functionalization of Colloidal Nanocrystals, Adv. Mater. 2017. 29, 1604878

[152] Andrew B. L., Thiol-ene “click” reactions and recent applications in polymer and materials synthesis, Polym. Chem. 2010. 1, 17-36

[153] Maarten v. D., Dirk T. S. R., Rob M. J. L., Cornelus F. v. N. and Wim E. H., Synthesis and Applications of Biomedical and Pharmaceutical Polymers via Click Chemistry Methodologies, Bioconjugate Chem. 2009. 20, 2001–2016

[154] Kazuo T. and Yoshiki C., Advanced functional materials based on polyhedral oligomeric silsesquioxane (POSS), J. Mater. Chem. 2012. 22, 1733-1746

[155] Hui Z., Qun Y. and Jianwei X., Polyhedral oligomeric silsesquioxane-based hybrid materials and their applications, Mater. Chem. Front., 2017. 1, 212—230

[156] Kai W. H. and Shiao W. K., High-Performance Polybenzoxazine Nanocomposites Containing Multifunctional POSS Cores Presenting Vinyl-Terminated Benzoxazine Groups, Macromol. Chem. Phys. 2010. 211, 2301–2311

[157] Siyu Q., Kunlin C.,Yunjie Y. and Chaoxia W., Robust UV-cured superhydrophobic cotton fabric surfaces with self-healing ability, Mat. and De. 2017. 116, 395-402

[158] Warintorn T., Xiaoshan F.,Yang S., Jayven C. C. Y., Du Y. and Chaobin H., Simultaneous enhancement of strength and toughness of epoxy using

doi:10.6342/NTU202101615

POSS-Rubber coreeshell nanoparticles, Com. Sci. and Tech. 2015. 118, 63-71

[159] Hongxia W., Hua Z., Adrian G., Jian F., Haitao N., Jie D. and Tong L., Robust, electro-conductive, self-healing superamphiphobic fabric prepared by one-step vapour-phase polymerisation of poly(3,4-ethylenedioxythiophene) in the presence of fluorinated decyl polyhedral oligomeric silsesquioxane and fluorinated alkyl silane, Soft Matter. 2013. 9, 277-282

[160] Yuwei Y., Dawei Z., Tong L., Zhiyong L., Wei L., Jibin P., Hao C., Haichao Z. and Xiaogang L., Improvement of anticorrosion ability of epoxy matrix in simulate marine environment by filled with superhydrophobic POSS-GO nanosheets, Jo. of Haz. Mat. 2019. 364, 244-255

[161] Junya Y., Zhaozhu Z., Mingming Y., Wenjing W., Xuehu M. and Weimin L., POSS grafted hybrid-fabric composites with a biomimic middle layer for simultaneously improved UV resistance and tribological properties, Comp. Sci. and Tech. 2018. 160, 69-78

[162] Yanchang G., Xuesong J. and Jie Y., Self-Wrinkling Patterned Surface of Photocuring Coating Induced by the Fluorinated POSS Containing Thiol Groups (F-POSS-SH) as the Reactive Nanoadditive, Macromolecules 2012. 45, 7520–7526

[163] Chao H. X., Qian Q. F., Xiao J. G., Qiu F. and Shun T. J., Fabrication of superhydrophobic cotton fabrics by grafting of POSS-based polymers on fibers, Appl. Sur. Sci. 2019. 465, 241-248

[164] Gaoyang L., Wei W. and Dan Y., Robust and self-healing superhydrophobic cotton fabric via UV induced click chemistry for oil/water separation, Cellulose 2019. 26, 3529-3541

doi:10.6342/NTU202101615

[165] Sahar F. and Mohammad M. Z., Fabrication of superhydrophobic coatings with self-cleaning roperties on cotton fabric based on Octa vinyl polyhedral oligomeric silsesquioxane/polydimethylsiloxane (OV-POSS/PDMS) nanocomposite, Jo. of Col. and Int. Sci. 2019. 540, 78-87

[166] Yifu Z., Yongyun M., Dongzhi C., Weibing W., Shengping Y., Shaobo M. and Chi H., Synthesis and characterization of addition-type silicone rubbers (ASR) using a novel cross linking agent PH prepared by vinyl-POSS and PMHS, Pol. Deg. and Stab. 2013. 98, 916-925

[167] Qiangyu Q.,Jun X.,,Mingzu Z., Jinlin H. and Peihong N., Versatile Construction of Single-Tailed Giant Surfactants with Hydrophobic Poly(ε-caprolactone) Tail and Hydrophilic POSS Head, Polymer 2019. 11(2), 311

[168] Abhishek N. M., Yubin H., Liang G., Liang W., Kamana E., Md. Masem H. and Tongwen X., Preparation and characterization of click-driven N-vinylcarbazole-based anion exchange membranes with improved water uptake for fuel cells, RSC Adv., 2017. 7, 29794-29805

[169] Shang Q., Liu C., Chen J., Yang X., Hu Y., Hu L., Zhou Y. and Ren X., Sustainable and Robust Superhydrophobic Cotton Fabrics Coated with Castor Oil-Based Nanocomposites for Effective Oil−Water Separation, ACS Sustainable Chem. Eng. 2020. 8, 7423–7435

[170] Hou K., Zeng Y., Zhou C., Chen J., Wen X., Xu S., Cheng J. and Pi P., Facile generation of robust POSS-based superhydrophobic fabrics via thiol-ene click chemistry, Chem. Eng. J. 2018. 33, 150−159

[171] Milne I, Ritchie RO, Karihaloo B. 2007. Comprehensive Structural Integrity, Elsevier, Amsterdam.

doi:10.6342/NTU202101615

[172] Al-Maliki H (2018) Adhesive and tribological behaviour of cold atmospheric plasma-treated polymer surfaces, 2018.10.14751/SZIE.2018.027

[173] Wang Z., Han M., Zhang J., He F., Xu Z., Ji S., Peng S. and Li Y., Designing preferable functional materials based on the secondary reactions of the hierarchical tannic acid (TA)-aminopropyltriethoxysilane (APTES) coating, Ch. Eng. Jo., 2019. 360(15), 299-312

[174] Sheng W., Li W., Yu B., Li B., Rainer J., Jia X. and Zhou F., Mussel-Inspired Two-Dimensional Freestanding Alkyl-Polydopamine Janus Nanosheets, Angew.Chem. Int. Ed. 2019. 58, 12018 –12022

[175] Li W, Tang X. Z., Zhang H. B., Jiang Z. G., Yu Z. Z., Du X. S. and Mai Y. W., Simultaneous surface functionalization and reductionvof graphene oxide with octadecylamine for electricallyconductive polystyrene composites, Carbon 2011. 49, 4724-4730

[176] Lui L., Shi H., Yu H., Zhou R., Yin J. and Luan S., One-Step Hydrophobicization of Tannic Acid for Antibacterial Coating on Catheters to Prevent Catheter-Associated Infections, Biomater. Sci. 2019. 7, 5035-5043

[177] Xu L. Q., Dicky P., Noeh K. G. and Kang E. T., Thiol Reactive Maleimido-Containing Tannic Acid for the Bioinspired Surface Anchoring and Post-Functionalization of Antifouling Coatings, ACS Sustainable Chem. Eng. 2016. 4, 4264−4272

[178] Célia F. F., Arménio C. S., A. Ramalho, Jorge F.J. C. and Ana C. F., Preparation of fully biobased epoxy resins from soybean oil based amine Hardeners, Ind. Cr. And Pro. 2017. 109, 434-444

[179] Xiong K., Qi P., Yang Y., Li X., Qiu H.,ab Li X., Shen R., Tu Q., Yang Z. and Huang N., Facile immobilization of vascular endothelial growth factor on a

doi:10.6342/NTU202101615

tannic acid-functionalized plasma-polymerized allylamine coating rich in quinone groups, RSC Adv., 2016. 6, 17188-17195

doi:10.6342/NTU202101615